

AD 717 771

STUDY OF SCATTERING AND FLUORESCENCE OF GASES  
IN THE VACUUM ULTRAVIOLET

F. M. Matsunaga, K. Watanabe, and W. Pong

Department of Physics and Astronomy  
University of Hawaii  
Honolulu, Hawaii 96822

Contract No. AF19(628)-4967

Project No. 8627

Task No. 862701

Work Unit No. 86270101

FINAL REPORT

Period Covered: 1 April 1965 through 30 September 1970

Date of Report - October 30, 1970

Contract Monitor: Robert E. Huffman, Aeronomy Laboratory

This document has been approved for public  
release and sale; its distribution is unlimited.

Prepared  
for

AIR FORCE CAMBRIDGE RESEARCH LABORATORIES  
AIR FORCE SYSTEMS COMMAND  
UNITED STATES AIR FORCE  
BEDFORD, MASSACHUSETTS 01730

# ABSTRACT

Measurements of spectral absorption and photoionization cross sections of  $\text{CO}_2$ ,  $\text{NH}_3$ ,  $\text{O}_2$ ,  $\text{COS}$ ,  $\text{NO}$ ,  $\text{N}_2$ , and vinyl chloride in the region 580 - 1650 Å were made. A number of new Rydberg series were found and the convergence limits were compared with the photoionization values.

In the study of dispersed fluorescence from molecules, particular attention was given to the emissions from  $\text{CO}$ ,  $\text{NH}_3$ ,  $\text{N}_2$ , and  $\text{NO}$  in the spectral region 1800 to 6000 Å. The experimental Franck-Condon factors for  $\text{CO}$  and  $\text{N}_2$  were found to be in good agreement with the theoretical values. The threshold for the  $\text{NH } c^1\Pi \rightarrow a^1\Delta$  transition was observed at  $(1245 \pm 10)$  Å. On the basis of the observed threshold of the  $\text{NH}$  emission, the calculated energy separation of the  $a^1\Delta$  state from the ground state of  $\text{NH}$  is  $(2.2 \pm 0.1)$  eV which is somewhat higher than the value previously reported. The excitation spectra of  $\text{NO}$  show many overlapping states. However, the  $\text{B}' \rightarrow \text{X}$  transitions of  $\text{NO}$  were identified, and the experimental Franck-Condon factors are in agreement with the calculated values. The results suggest that the  $\gamma'$  band contribution in  $\text{NO}$  emission is negligible. The excitation spectra of other molecules such as  $\text{H}_2$ ,  $\text{O}_2$ , and  $\text{SO}_2$  were studied, and certain features of the emission spectra can be related to the spectral absorption.

The effect of molecular collisions on the fluorescence of  $\text{NO}$  was investigated. Quenching of the  $\text{B}'$ ,  $\text{D}$ ,  $\text{E}$ , and  $\text{F}$  states with the enhancement of the  $\gamma$  band emission was observed.

LIST OF CONTRIBUTORS

Kanemura, D.	--	Assistant in Physics.
Matsunaga, F. M.	--	Junior Physicist.
Mori, K.	--	Associate Physicist. Presently at Institute for Physical and Chemical Research, Japan.
Nakata, R. S.	--	Assistant in Physics.
Pong, W.	--	Professor of Physics and Principal Investigator (1 April 1970 to present).
Sakai, H.	--	Presently at AFCRL.
Sood, S. P.	--	Associate Professor of Chemistry.
Watanabe, K.	--	Senior Professor of Physics and Principal Investigator (deceased 15 August 1969).
Yokotake, G.	--	Junior Specialist in Physics. Presently at Division of Weights and Measures, State of Hawaii.

#### ACKNOWLEDGMENTS

We are indebted to Dr. Y. Tanaka and Professor M. Ogawa for reproductions of their photographs of the COS and N<sub>2</sub> spectrograms. Special thanks are due to all the student assistants who have contributed much effort to the project. The assistance of Mr. Roy Tom in constructing some of our experimental apparatus is gratefully acknowledged.

# TABLE OF CONTENTS

	PAGE
1. INTRODUCTION. . . . .	1
2. ABSORPTION AND PHOTOIONIZATION STUDIES. . . . .	2
2.1 Publications . . . . .	8
2.2 Abstracts of Publications. . . . .	9
2.3 Rydberg Series of $N_2^+(A^2\Pi_u)$ . . . . .	12
3. FLUORESCENCE OF MOLECULES . . . . .	22
3.1 Introduction . . . . .	22
3.2 Theory of Absorption and Emission. . . . .	25
3.3 Experimental Details . . . . .	32
3.4 Relating Measured Emissions to Franck-Condon Factors . . . . .	36
3.5 Carbon Monoxide. . . . .	37
3.6 Ammonia. . . . .	46
3.7 Nitric Oxide . . . . .	52
3.8 Hydrogen, Nitrogen, Oxygen, and Sulfur Dioxide. . . . .	70
4. EFFECT OF MOLECULAR COLLISIONS ON FLUORESCENCE. . . . .	76
4.1 Introduction . . . . .	76
4.2 Inelastic Collisions and Quenching . . . . .	77
4.3 Effect of $N_2$ and Argon on Fluorescence of NO . . . . .	79
5. CONCLUDING REMARKS . . . . .	91

## 1. INTRODUCTION

Although extensive studies on gases in the vacuum uv region have been made, some emission characteristics of atmospheric gases under ultraviolet excitation are still not completely understood. In order to develop a better understanding of the physical processes that might generate the observed emissions, a program of vacuum uv experiments on simple molecules was initiated by the late Professor Kenichi Watanabe. The study involved the following laboratory measurements: 1) absorption and scattering of vacuum ultraviolet radiation; 2) photoionization of gases; 3) fluorescence of molecules under uv excitation. Particular attention was given to the ultraviolet absorption and photoionization properties of the following gases:  $N_2$ ,  $O_2$ ,  $NH_3$ ,  $COS$ ,  $CO$ ,  $CO_2$ , and  $NO$ . A special effort was made to investigate the weak dispersed fluorescence of simple molecules and to determine the effect of molecular collisions on the emission process.

The principal objectives of the experiments were to obtain experimental data for the identification of Rydberg and vibrational states, and for comparisons with theoretical parameters such as Franck-Condon factors and quenching cross-sections associated with molecular collisions. It was hoped that an experimental study of the effect of molecular collisions on fluorescence would lead to a better understanding of electronic energy transfer between molecules.

## 2. ABSORPTION AND PHOTOIONIZATION STUDIES

A significant part of our vacuum uv research has been the experimental study of absorption and photoionization of gases. Measurements of spectral absorption and photoionization cross sections of  $\text{CO}_2$ ,  $\text{NH}_3$ ,  $\text{O}_2$ ,  $\text{COS}$ ,  $\text{NO}$ , and vinyl chloride in the region 580-1650 Å were reported in several publications. The abstracts of these papers are presented in section 2.2 of this report.

The absorption and photoionization cross sections of atmospheric molecules in the spectral region 600-2000 Å are of current interest. In this region, the absorption curves show considerable band structures corresponding to electronic, vibrational, and rotational transitions. Continuous absorption bands and the underlying continua due to repulsive states leading to dissociations are also observed in these curves. In the absence of complex structures associated with overlapping bands, Rydberg transitions converging to the first ionization potential and higher potentials can be identified. Much of our recent work was performed with improved resolution in an effort to find new Rydberg series and to compare the convergence limits with the photoionization values. A detailed discussion of the results can be found in the papers listed in the following section of this report.

While the results of our absorption measurements showed

agreement with some previous work, there were noticeable discrepancies. Many of the previous errors may be due to pressure determination of the flowing gas. Perhaps it is worthwhile to describe the experimental conditions in which our measurements were made.

Two one-meter, normal-incidence monochromators, each with a 1200 lines/mm grating, were used in the experiments. Monochromator A (radius-mount type, built by McPherson Instrument) provided a resolution of  $0.2 \text{ \AA}$  with  $20 \mu$  slits and was used for the region 850-1700  $\text{\AA}$ . Monochromator B (Johnson-Onaka type, fabricated in our shop) had a three-stage differential-pumping system at the entrance slit and was used for the region 580-1000  $\text{\AA}$  with a helium light source. A resolution of about  $0.3 \text{ \AA}$  was obtained with slit widths of 30 and  $20 \mu$ , respectively, for the entrance and exit slits. The grating mount was coupled to a flexible cable to permit focusing under operating conditions.

A windowless hydrogen discharge tube was used with Monochromator A. It was operated at 0.35 or 0.4 amp dc with about 800 V across the tube. For the region 580-1000  $\text{\AA}$ , the Hopfield continuum which has been ascribed to emission from molecular helium was used as a light source for Monochromator B.

The helium light source and the entrance-slit section are schematically shown in Fig. 1. The capacitor C ( $0.0018 \mu\text{F}$ ) and the spark gap G including a small mercury lamp (not shown) were mounted within the light-source assembly and shielded. The resistor R ( $90 \text{ k}\Omega$ ) was placed inside a 20 kV Manson dc power



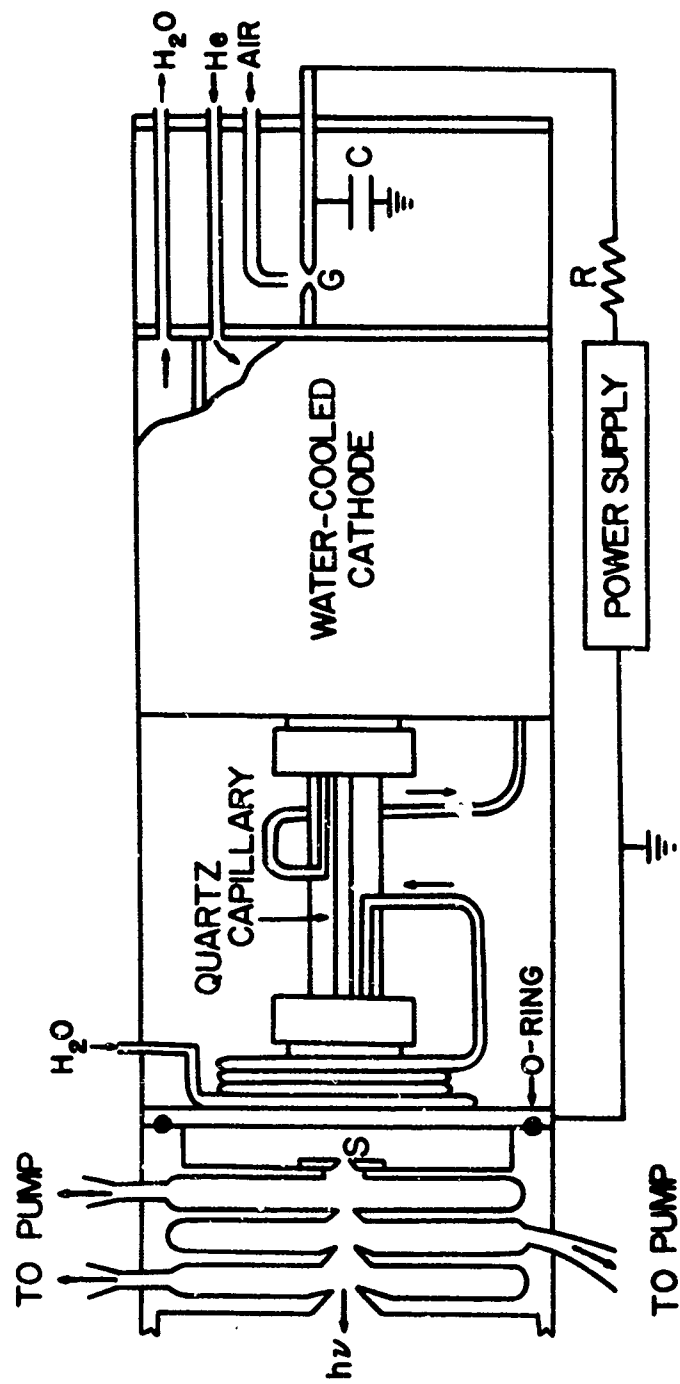


Fig. 1 (Sec. 2). Schematic diagram of light source and differential pumping slits.

supply (Model 605) and connected to the light source by a cable. The tungsten electrodes of the spark gap were attached to lucite rods in such a manner that the gap distance can be adjusted during operation of the light source. The repetition rate of gap breakdown was about 6 kc. Commercial (medical) grade helium was flowed through a copper foil trap and a liquid-nitrogen trap to the light source and was pumped out through the optical slit (S in Fig. 1) via the 3-stage pumping system. For most measurements the pressure was about 120 mm Hg in the light source and  $10^{-5}$  mm Hg in the main chamber of the monochromator. The photon flux through the exit slit was determined by a xenon ion chamber, using our recent result that photoionization yield of xenon is unity, and found to be about  $2 \times 10^7$  photons/sec through the exit slit at the peak (810 Å) of the Hopfield continuum.

Absorption coefficients were measured by a method described in our earlier publications. The absorption chamber was located between the exit slit and a glass plate coated with sodium salicylate, and an EMI - 9514B photomultiplier tube was placed in air a few mm behind the glass plate. An absorption cell of length 10.5 cm with LiF windows and parallel plate electrodes was used for the region above 1070 Å. For shorter wavelengths the exit slit served as the window, and absorption path lengths of 11.5, 13.6, 27.1 and 54 cm were used.

Photoionization yields were determined by comparing the ion current of a given gas with that of a reference gas with known

yield. For the region above  $1070 \text{ \AA}$ , the cell with LiF windows was used with nitric oxide as a reference gas. To insure total absorption in the ion chamber, relatively high gas pressures were used. For the region below  $1020 \text{ \AA}$ , an ion chamber of length  $54 \text{ cm}$  was used with xenon as a reference gas. For most measurements the gas pressures were high enough to give total absorption; however, a photomultiplier placed at the end of the ion chamber continuously measured any transmitted light so that corrections can be applied.

In order to have a negligible pressure gradient in a flow type absorption chamber, a small exit slit ( $0.02 \times 10 \text{ mm}$ ) and large chamber dimensions ( $15 \text{ cm}$  diameter and  $54 \text{ cm}$  length) were used. Moreover, the chamber was opened to a side chamber of  $6 \text{ liter}$  volume. A Consolidated micromanometer was connected directly to the absorption chamber. The pressure calibration curve for the manometer obtained with this arrangement was the same as those obtained with shorter cell lengths. In each case the calibration curve was obtained by the following two methods: (a) McLeod gauge using static gas ( $\text{O}_2$ ,  $\text{N}_2$ , or air) and (b) absorption method using oxygen flowing through the absorption chamber. Calibration curves were obtained from time to time in order to detect any change in the sensitivity of the micromanometer. A typical calibration curve is shown in Fig. 2. The error in our pressure determination is estimated to be less than  $5\%$ .

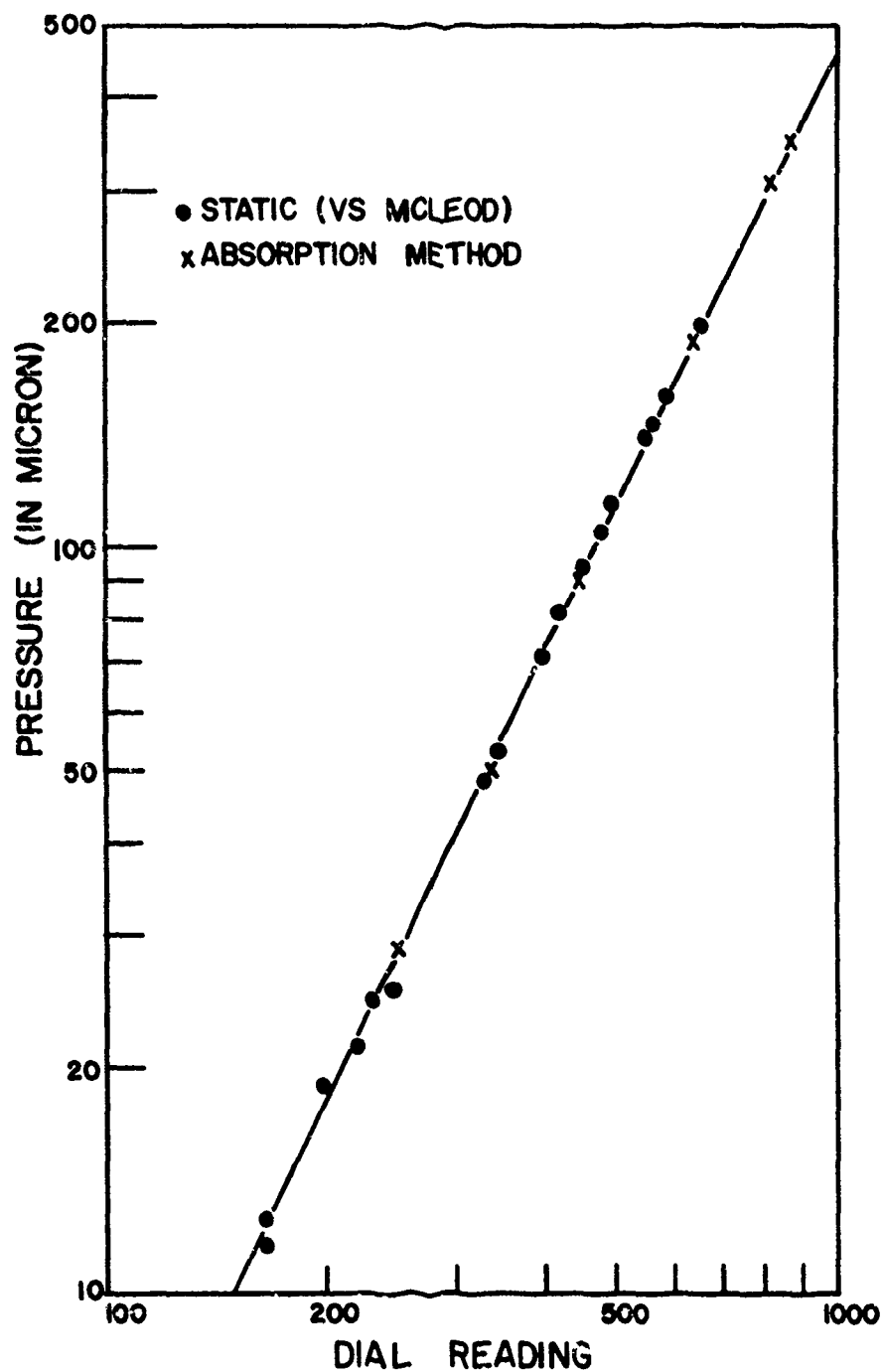


Fig. 2 (Sec. 2). Pressure calibration curve for Consolidated micromanometer.

## 2.1 PUBLICATIONS PREPARED UNDER CONTRACT AF 19 (628) - 4967

1. "Absorption and Photoionization Coefficients of  $\text{CO}_2$  in the Region 580-1670 Å"  
by R. S. Nakata, K. Watanabe, and F. M. Matsunaga  
Science of Light, Vol. 14, 54 (1965).
2. "Absorption and Photoionization Coefficients of  $\text{NH}_3$  in the 580-1650 Å Region"  
by K. Watanabe and S. P. Sood  
Science of Light, Vol. 14, 36 (1965).
3. "Absorption and Ionization Coefficients of Vinyl Chloride"  
by S. P. Sood and K. Watanabe  
The Journal of Chemical Physics, Vol. 45, 2913 (1966).
4. "Ionization Potential and Absorption Coefficient of COS"  
by F. M. Matsunaga and K. Watanabe  
The Journal of Chemical Physics, Vol. 46, 4457 (1967).
5. "Total and Photoionization Coefficients and Dissociation Continua of  $\text{O}_2$  in the 580-1070 Å Region"  
by F. M. Matsunaga and K. Watanabe  
Science of Light, Vol. 16, 31 (1967).
6. "Absorption Coefficient and Photoionization Yield of NO in the Region 580-1350 Å "  
by K. Watanabe, Frederick M. Matsunaga, and Hajime Sakai  
Applied Optics, Vol. 6, 391 (1967).

## 2.2 ABSTRACTS OF PUBLICATIONS

### 1. Absorption and Photoionization Coefficients of $\text{CO}_2$ in the Region 580-1670 Å

Absorption coefficient of  $\text{CO}_2$  in the region 580-1670 Å and photoionization yield in the region 580-900 Å were obtained by photoelectric techniques with improved resolution. Hopfield helium continuum and hydrogen sources were used. Photoionization efficiencies ranged from 60 to 95% and most bands were found to be preionized. The doublet ionization potentials (13.786 and 13.766 eV) were confirmed by the photoionization curve.

### 2. Absorption and Photoionization Coefficients of $\text{NH}_3$ in the 580-1650 Å Region

Absorption coefficient of  $\text{NH}_3$  gas in the region 580-1650 Å and photoionization yield in the region 580-1220 Å were determined by photoelectric techniques. The Hopfield helium continuum was used as source for the region 580-1000 Å with 0.3 Å resolution and the hydrogen source for the region 850-1650 Å with 0.2 Å resolution. The improved resolution yielded finer details in the absorption curve for the region above 1150 Å. On the basis of Rydberg band analysis, the first ionization potential appears to be 10.166 eV, which is consistent with photoionization measurements.

### 3. Absorption and Ionization Coefficients of Vinyl Chloride

Absorption coefficients of vinyl chloride were measured by a photoelectric method at many wavelengths in the region 1075-2000 Å, and photoionization yields were obtained in the region 1075-1240 Å with an ion chamber. Many bands were identified as members and their vibrational companions of four Rydberg series and one other electronic transition. These Rydberg series and the photoionization curve yielded the same ionization potential of  $10.00 \pm 0.01$  eV.

### 4. Ionization Potential and Absorption Coefficient of COS

Absorption and photoionization coefficients of COS in the region 1070-1700 Å were measured with a resolution of 0.5 Å by photoelectric methods. The absorption curves support the photographic studies of Price and Simpson and Tanaka, Jursa, and LeBlanc. The doublet first ionization potential of the molecule was found to be 11.18 and  $11.22 \pm 0.01$  eV from the convergence limit of a Rydberg series and the photoionization curve.

### 5. Total and Photoionization Coefficients and Dissociation Continua of O<sub>2</sub> in the 580-1070 Å Region

Absorption coefficients and photoionization yields of O<sub>2</sub> have been measured in the 580-1070 Å region using the Hopfield helium continuum as background with 0.3 Å resolution

and the  $H_2$  emission source in the 900-1070 Å region with 0.2 bandwidth. By subtracting the absorption due to discrete bands and photoionization processes from the total absorption coefficient, it was possible to uncover four dissociation continua which appear to be consistent with predicted dissociation energies of  $O_2$ .

6. Absorption Coefficient and Photoionization Yield of NO in the Region 580-1350 Å

Photoionization yield and absorption coefficient of nitric oxide were measured at many wavelengths in the region 580-1350 Å.  $H_2$  emission and helium continuum sources were used with a 1-m monochromator. Absolute intensity measurements were based on a calibrated thermocouple.



### 2.3 Rydberg Series Converging to $N_2^+(A^2\Pi_u)$ .

#### Abstract

Absorption and photoionization coefficients of  $N_2$  in the region 700 to 800 Å were measured with a resolution of 0.3 Å by photoelectric methods. The absorption curves are consistent with the photographic plates of Ogawa. An additional Rydberg series converging to the  $A^2\Pi_u$  state of  $N_2^+$  is proposed.

#### Introduction

The electronic spectra of the nitrogen molecule have been studied extensively in recent years. In the last decade a number of important experimental and theoretical papers have appeared.<sup>1-12</sup> Mulliken<sup>2</sup> has assigned electron configurations to about 100 states, most of which have not yet been observed. Dressler<sup>12</sup> has surveyed the interaction of the lowest valence and Rydberg series of  $N_2$ . Ogawa and Tanaka<sup>3</sup> reported several Rydberg series converging to  $A^2\Pi_u$  of  $N_2^+$  in the spectral region 700-800 Å. Another Rydberg series involving the (ndσ) orbital is expected to converge to  $A^2\Pi_u$  state.<sup>9</sup> In this region of interest, the absorption and photoionization coefficients have been measured by several investigators.<sup>13-16</sup>

In the present work, the absorption and photoionization coefficients obtained with improved resolution of about 0.3 Å in the region 700-800 Å are reported. In addition, a reassignment of several bands into a Rydberg series converging to  $A^2\Pi_u$  state is discussed.

### Experimental

The apparatus and experimental procedures used for this study have been described in a previous paper.<sup>17</sup> A one-meter vacuum monochromator (Johnson-Onaka mount) with a three-stage differential-pumping system at the entrance slit was used. With a Hopfield helium continuum source, dispersed radiation in the spectral region (580-1000 Å) was obtained. The measurements were made with a resolution of about 0.3 Å. The absorption chamber was located between the exit slit and a glass plate coated with sodium salicylate, and an EMI - 9514B photomultiplier tube was placed in air a few mm behind the glass plate.

The N<sub>2</sub> and Xe gas samples were assayed reagent grade from Matheson Company. Gas pressures in the absorption chamber were measured with a Consolidated micromanometer as described<sup>17</sup> previously. The error in our pressure measurement was estimated to be less than 5%. Pressures of gas used for the k-value measurements were as follows: 0.02 to 1.0 Torr in an 11.5 cm windowless cell. For photoionization measurements pressures of 0.02 to 1.0 mm Hg used in a 54 mm cell were adequate for total absorption of light by N<sub>2</sub> and by xenon.

The photoionization yield of N<sub>2</sub> was obtained by comparing the ion current of N<sub>2</sub> with that of xenon which has been found<sup>18,19</sup> to have a photoionization yield of unity in the region below 1020 Å. The small corrections for scattered light were made at most wavelengths. In our arrangement, the fluorescence of N<sub>2</sub>

could not be detected, and the corrections such as used by Huffman, et al.<sup>20</sup> were not necessary.

The experimental error in the  $k$ -values at most wavelengths was estimated to be about 10%. The experimental error in the ionization yield was about 10% for most wavelengths. Furthermore, there was some uncertainty in the yield value at the center of some strong sharp bands due to inadequate resolution.

The absorption coefficient or  $k$ -value in  $\text{cm}^{-1}$  is defined by the equation  $I = I_0 \exp(-kx)$ , where  $I_0$  and  $I$  are the incident and transmitted intensities and  $x$  in cm is the layer thickness of the gas reduced to 1 atm pressure and  $0^\circ \text{C}$ . The photoionization coefficient is defined by  $k_i = kY$ , where  $Y$  is the fractional yield of photoionization.

#### A. Absorption Coefficients and Photoionization Yields of $\text{N}_2$

Mean absorption coefficients and photoionization yields are summarized in Fig. 1. The upper curve represents the photoionization yield values in per cent, while the lower one shows the absorption coefficients of  $\text{N}_2$ . The designations of the series and progressions are the same as used by Ogawa.<sup>4</sup>

The details of the absorption spectrum shown in Fig. 1 are in good agreement with those obtained by previous investigators,<sup>14-16</sup> who used the helium continuum as background. Comparisons of the present results with others are limited to the relatively recent papers of Huffman, et al.,<sup>14</sup> Cook and Ogawa,<sup>16</sup> and Samson and

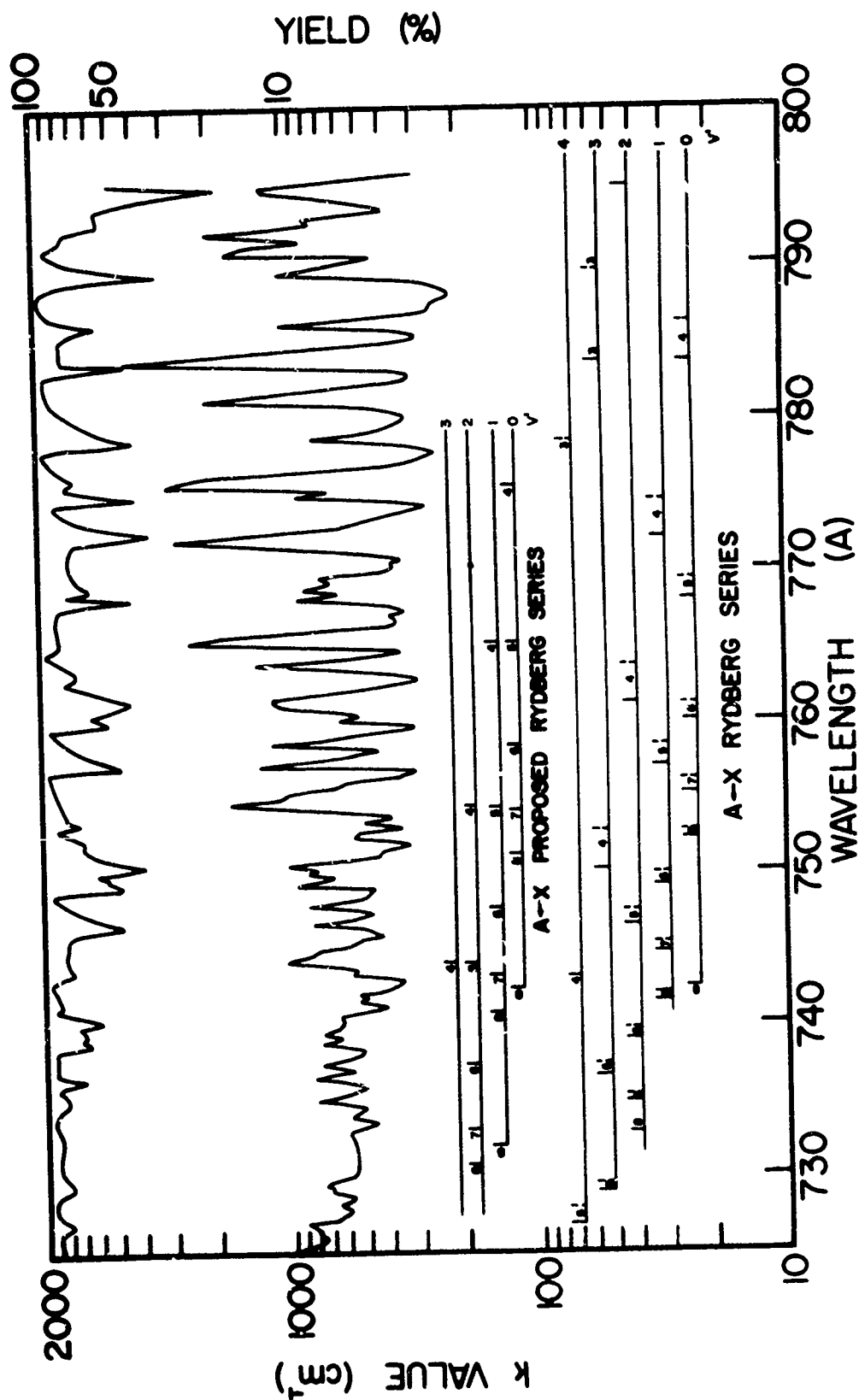


Fig. 1 (Sec. 2.8). Absorption coefficient and photoionization yield curve of  $N_2$  in the region 730 to 800 Å.

Cairns.<sup>21</sup> Huffman, et al.<sup>14</sup> have compared their results in considerable detail with earlier results reviewed by Watanabe.<sup>22</sup>

Compared to the results of Huffman, et al.<sup>14</sup> our k-values are in good agreement but some discrepancies of 25% occur at some wavelengths and our k-values are generally lower. While our results are in better agreement with those of Cook and Ogawa,<sup>16</sup> there are some differences: the k-values from our measurements are higher at band maxima and lower at the minima. Our k-values are in best agreement with those of Samson and Cairns.<sup>21</sup> At about 12 wavelengths where comparisons can be made, the k-values agreed within about 10%. The present photoionization yields agreed within 15% with those of Samson and Cairns,<sup>21</sup> and within 15% with most wavelengths and up to 25% for others of Cook and Ogawa.<sup>16</sup>

#### B. Rydberg Series Which Converges to the $A^2\Pi_u$ State of $N_2^+$

In the region 725 to 800 Å there are many bands belonging to Rydberg series converging to  $v' = 0, 1, 2, 3$ , and 4 levels of the  $A^2\Pi_u$  state of  $N_2^+$ .<sup>3,23</sup> Electronic configuration and the electronic states assigned to these series are as follows:

$$KK (\sigma_g 2s)^2 (\sigma_u 2s)^2 (\Pi_u 2p)^3 (\sigma_g 2p)^2 (ns\sigma), {}^1\Pi_u \text{ and } {}^3\Pi_u.$$

Another Rydberg series with an electronic configuration,

$$KK (\sigma_g 2s)^2 (\sigma_u 2s)^2 (\Pi_u 2p)^3 (\sigma_u 2p)^2 (nd\sigma),$$

and electronic state of  ${}^1\Pi_u$  which converges to the  $A^2\Pi_u$  state of  $N_2^+$  is expected in this wavelength region.<sup>3</sup> Recently, Lefebvre-Brion and Moser<sup>9</sup> predicted that the first member of the Rydberg series of the type  $(nd\sigma) {}^1\Pi_u \leftarrow X^1\Sigma_g^+$  to be at about  $1600 \text{ cm}^{-1}$  higher than that of the first observed member of the  $(nsc) {}^1\Pi_u \leftarrow X^1\Sigma_g^+$  series which is located at 15.15 eV above the ground state.<sup>24</sup>

The absorption coefficient (k-value) curve in Fig. 1 is labeled similarly to that of Ogawa.<sup>4</sup> The solid vertical lines represent Worley's Third Rydberg series, and the dashed lines are the Ogawa and Tanaka Rydberg series. The upper states of the former belong to  ${}^1\Pi_u$ , and the latter is associated with  ${}^3\Pi_u$ . Our absorption curve and the spectrogram of Ogawa show the strong and diffuse bands of several new progressions observed by Ogawa.<sup>4</sup> These bands of the progressions can be reassigned to fit the Rydberg series converging to  $v' = 0, 1, 2$ , and 3 levels of the  $A^2\Pi_u$  state of  $N_2^+$ , as shown in Table I. The proposed Rydberg series for  $v' = 0$  is

$$\nu_m = 134725 - \frac{R}{(m + 0.25)^2}, \text{ where } m = 4, 5, 6, 7, 8.$$

The band head wave numbers and series limits (SL) are taken from Ogawa,<sup>4</sup> and are listed with the effective principal quantum number  $n^*$ . The 4th members of the proposed Rydberg series belonged to the Ogawa P(1) progressions. The 5th members are considered to be overlap from the P(1) progression, i.e., 4th member of

Table I

Rydberg Series Converging to  $A^2\Pi_u^+$  of  $N_2^+$ .

m	$v' = 0$		$v' = 1$		$v' = 2$		$v' = 3$	
	$\nu_{\text{obs.}}$ ( $\text{cm}^{-1}$ )	$n^*$	$\nu_{\text{obs.}}$ ( $\text{cm}^{-1}$ )	$n^*$	$\nu_{\text{obs.}}$ ( $\text{cm}^{-1}$ )	$n^*$	$\nu_{\text{obs.}}$ ( $\text{cm}^{-1}$ )	$n^*$
4	128892	4.34	130741	4.33	132584	4.33	134392	4.33
5	130741	5.25	132584	5.23	134392	5.21		
6	131906	6.24	133770	6.23	135589	6.21		
7	132650	7.27	134523	7.28	136366	7.27		
8	133119	8.265	134984	8.25	136820	8.23	138635	8.23
	SL = 134725 $\text{cm}^{-1}$		SL = 136595 $\text{cm}^{-1}$		$\bar{\nu} = 138440 \text{ cm}^{-1}$		SL = 140255 $\text{cm}^{-1}$	

$v' = 1$  overlaps with 5th member of  $v' = 0$ , and so forth. The high absorption intensity and diffuseness of these bands may indicate overlap of their members. The 6th, 7th, and 8th members are members of  $P(2)$ ,  $P(3)$ , and  $P(4)$ , respectively. Ogawa<sup>4</sup> listed several unidentified bands and these may belong to the 3rd members of the proposed series. The 8th member is accompanied by another band separated about  $40 \text{ cm}^{-1}$  to the longer wavelength side. This is similar to the series reported by Ogawa<sup>4</sup> and may converge to  $A^2\Pi_{u,3/2}$ . The lowest member of the Rydberg series was expected to be in the  $810 \text{ \AA}$  region which agrees with the prediction of Lefebvre-Brion and Moser for  $(4d\sigma)$  transitions to higher  $^1\Pi_u$  states. There are several strong and diffuse bands in this region of  $124000$  to  $125000 \text{ cm}^{-1}$  and again overlap is possible for the lowest member of the Rydberg series. Further high resolution investigation of the absorption spectrum is necessary in order to establish the position of the lowest member of the Rydberg state  $^1\Pi_u$ .



References

1. A. Lofthus, "The Molecular Spectrum of Nitrogen", Spectroscopic Report No. 2, University of Oslo, 1960.
2. R. A. Mulliken, "Threshold of Space", page 169, Pergamon Press, N. Y., 1957.
3. M. Ogawa and Y. Tanaka, Cand. J. Phys. 40, 1593 (1962).
4. M. Ogawa, Cand. J. Phys. 42, 1087 (1964).
5. D. Mahon-Smith and P. K. Carroll, J. Chem. Phys. 41, 1377 (1964).
6. M. Ogawa, Y. Tanaka and A. S. Jursa, Cand. J. Phys. 42, 1716 (1964).
7. P. K. Carroll and K. Yoshino, J. Chem. Phys., 47, 3073 (1967).
8. P. K. Carroll and C. P. Collins, Cand. J. Phys., 47, 563 (1969).
9. H. Lefebvre-Brion and C. M. Moser, J. Chem. Phys., 43, 1394 (1965).
10. Paul E. Cade, K. D. Sales, and A. C. Wahl, J. Chem. Phys., 44, 1973 (1966).
11. R. C. Sahni and B. C. Sawhney, Int. J. Quantum Chem. 1, 251 (1967).
12. K. Dressler, Cand. J. Phys., 47, 547 (1969).
13. R. E. Huffman, Y. Tanaka, and J. C. Larrabee, J. Chem. Phys. 38, 1920 (1963).
14. R. E. Huffman, Y. Tanaka, and J. C. Larrabee, J. Chem. Phys. 39, 910 (1963).

15. G. R. Cook and P. H. Metzger, J. Chem. Phys. 41, 321 (1964).
16. G. R. Cook and M. Ogawa, Cand. J. Phys. 43, 256 (1965).
17. K. Watanabe and S. P. Sood, Science of Light, 14, 36 (1965).
18. J. A. R. Samson, J. O. S. A., 54, 6 (1964).
19. F. M. Matsunaga, R. S. Jackson and K. Watanabe, J. Q. S. R. T.,  
5, 329 (1965).
20. R. E. Huffman, J. C. Larrabee and Y. Tanaka, J. Chem. Phys.  
40, 356 (1964).
21. J. A. R. Samson and R. B. Cairns, J. G. R. 69, 4583 (1964).
22. K. Watanabe, Adv. Geophys. 5, 153 (1958).
23. R. E. Worley, Phys. Rev. 64, 207 (1943); Phys. Rev. 89,  
(1953).

### 3. FLUORESCENCE OF MOLECULES

#### 3.1 Introduction

Laboratory studies on fluorescence of gases and vapors were initiated in the early part of the present century.<sup>1</sup> Mitchell and Zemansky<sup>2</sup> have reported some results prior to 1933. The first attempt to wavelength-analyze both the exciting radiation and fluorescence was made by Meyer<sup>3</sup> in studying nitrogen excited by radiation from a spark. Due to atmospheric and window absorption this work was limited to the region above 1000 Å. During more recent times, considerable effort has been directed in obtaining fluorescence data on many hydrocarbon and other complicated molecules.<sup>4,5</sup>

Recently, spectroscopic study of fluorescence from various atmospheric molecules excited by emission line spark source between 500-1000 Å was reported.<sup>6-8</sup> The fluorescence was observed in the 3500-6500 Å region. Several investigators have used rare gas resonance and H<sub>2</sub> emission light sources to excite, photoionize and photodissociate simple molecules in the 1000-2000 Å range to study the resulting fluorescence.<sup>9,10</sup> Primarily, narrow and broadband filters were used to analyze the emission. Carrington,<sup>11</sup> Young, et al,<sup>12</sup> and Callear and Smith<sup>13</sup> utilized spectrometers to study the fluorescence spectra in the spectral region of 1800-7500 Å.

In the study of fluorescence from diatomic and polyatomic

molecules, we can observe emission from atoms, diatomic molecules, radicals, and polyatomic molecules produced by photoexcitation, dissociation and ionization. Photon-impact method with monochromatic radiation is more useful than electron impact because a discrete state can be populated. Monoenergetic electrons are difficult to produce in the 6 to 12 eV region. If higher energy electrons are used, the emission spectra of the molecules would be too complicated to analyze.

In the case of atoms some theoretical transition probabilities are available.<sup>14</sup> For molecules, however, the results of calculations are meager. Since molecules undergo electronic, vibrational and rotational transitions, the dipole matrix is difficult to calculate. In spite of the mathematical difficulties, some theoretical work has been done on the assumption that a slow vibrational or rotational motion of the molecules should have little effect on the electronic state of the molecule. The motion may distribute the light intensity associated with the ideal electronic lines over many lines or over a broad continuum. According to the approximation of Born and Oppenheimer,<sup>15</sup> the form of this distribution is decided by the Honl-London (rotational)<sup>16</sup> and Franck-Condon (vibrational)<sup>17</sup> factors. The band intensities for most diatomic molecules can be related to the Franck-Condon factors calculated from the Schrodinger wave equation using the Morse<sup>18</sup> and more recently, R-K-R type potentials.<sup>19</sup> Since the Franck-Condon factors have been calculated for some

molecules,<sup>19-23</sup> it would be desirable to measure the emission of these molecules and compare the results with those of calculations.

### 3.2 Theory of Absorption and Emission

The absorption coefficient  $k$  in  $\text{cm}^{-1}$  is defined by the equation

$$I = I_0 \exp(-kx),$$

where  $I_0$  and  $I$  are the incident and transmitted light intensities and  $x$  in  $\text{cm}$  is the layer thickness of the absorbing gas reduced to  $273^\circ \text{K}$  and  $1 \text{ atm}$  pressure. The absorption cross section  $\sigma$  in  $\text{cm}$  is defined by

$$\sigma = k/n_0,$$

where  $n_0$  is Loschmidt's number ( $2.69 \times 10^{19}$  particles per  $\text{cm}^3$ ).

The photoionization cross section  $\sigma_i$  is defined by

$$\sigma_i = \sigma Y,$$

where  $Y$  is the quantum yield of photoionization. If the  $k$ -values are known throughout the spectral region covered by a particular electronic transition, the oscillator strength or  $f$ -value of this transition can be computed by

$$f = \frac{mc^2}{\pi e^2 n_0} \int_{\nu_1}^{\nu_2} k d\nu,$$

where  $e^2/mc^2$  is the classical electron radius and  $\nu$  is the wave number in  $\text{cm}^{-1}$ . Various sum rules are associated with the  $f$ -value and provide checks on the accuracy and validity of theoretical calculations involving cross sections. Of importance is the sum rule which states that, for a single electron, the  $f$ -values for

all possible transitions will add up to unity, i.e.,  $\sum f = 1$ , and correspondingly, when  $Z$  electrons are involved in the absorption, i.e.,  $\sum f = Z$ . The oscillator strength is related to Einstein coefficient  $A$  in  $\text{sec}^{-1}$  for spontaneous emission by the equation

$$f_{lu} = \frac{mc}{8\pi^2 e^2 \nu^2} \cdot \frac{g_u}{g_l} A_{ul},$$

where  $g_u$  and  $g_l$  represent degeneracies of the upper and lower states, respectively. The Einstein coefficient for absorption  $B$  is related to  $A$  by

$$A_{ul} = 8h\nu^3 \pi \frac{g_l}{g_u} \cdot B_{lu}.$$

The radiative lifetime  $\tau_u$  of the upper state is related to Einstein  $A$  coefficients by

$$\frac{1}{\tau_u} = \sum_l A_{ul}.$$

For electric dipole transitions,<sup>18</sup>  $A$  and  $B$  coefficients are related to a transition strength  $S_{ul}$  in the following equations:

$$A_{ul} = \frac{64\pi^4 \nu^3}{3hg_u} \cdot S_{ul},$$

and

$$g_u B_{ul} = g_l B_{lu} = \frac{8\pi^3}{3h^2} \cdot S_{ul}.$$

For electric dipole transitions the transition strength is defined by

$$S_{ul} = \left| \int \psi_u^* M \psi_l dv \right|^2,$$

where  $\Psi_u$  and  $\Psi_l$  are the complete wave functions of the u and l states and  $dv$  is the element of configuration space involved.  $M$  is the electric dipole moment of the transition, with

$$M^2 = M_x^2 + M_y^2 + M_z^2,$$

and

$$M_x = e \sum_i x_i,$$

the sum being taken over all electrons  $i$ .

The previous equations concerning A and B which hold for specific transitions between pairs of atomic levels also hold formally for the  $U, v', J' \rightarrow L, v'', J''$  molecular transitions.<sup>18,21</sup> In the case of vibronic transitions  $v' \rightarrow v''$  where the molecular bands are sufficiently narrow that a realistic value of  $\nu_{v',v''}$  and  $S_{v',v''}$  may be assigned to it. The Einstein coefficient  $A_{v',v''}$  for the  $v', v''$  band of an electric dipole system is given by

$$A_{v',v''} = \frac{64\pi^4 \nu^3(v',v'')}{3h g_u} \cdot S_{v',v''}.$$

The band strength  $S_{v',v''}$  is defined by

$$S_{v',v''} = \left| \int \Psi_{v'} R_e(r) \Psi_{v''} dr \right|^2,$$

where  $\Psi_{v'}$  and  $\Psi_{v''}$ , the vibrational wave functions of the  $v'$  and  $v''$  levels, are each solutions of a one-dimensional wave equation.

The wave equation is

$$\frac{d^2 \Psi}{dr^2} + \frac{8\pi\mu}{h^2} [E_v - U(r)] \Psi = 0,$$



where  $r$  is the internuclear separation of the molecule and  $\mu$  the reduced mass.  $E_v$  is the energy eigenvalue of the  $v$ 'th level and  $U(r)$  is the molecular potential. The electronic transition moment of the band system is defined by

$$R_e(r) = \int \psi_{eu}^* M \psi_{el} dV,$$

where  $\psi_{eu}$  and  $\psi_{el}$  are molecular wave functions. The electronic transition moment has been difficult to calculate. Under suitable conditions and for most band systems,<sup>24</sup> it is possible to rewrite the band strength equation as

$$S_{v'v''} = R_e^2(\bar{r}) \left| \int \psi_{v'} \psi_{v''} dr \right|^2 = R_e^2(\bar{r}) q(v'v''),$$

where the vibrational overlap integral squared

$$q(v'v'') = \left| \int \psi_{v'} \psi_{v''} dr \right|^2$$

is called the Franck-Condon factor of the band. The Franck-Condon factors for a band are normalized according to

$$\sum_{v'} q(v'v'') = \sum_{v''} q(v'v'') = 1.$$

The  $r$ -centroid

$$\bar{r} = \int \psi_{v'} \psi_{v''} r dr / \int \psi_{v'} \psi_{v''} dr$$

is a characteristic internuclear separation associated with the band. The band oscillator strength  $f_{v'v''}$  is

$$f_{v'v''} = \frac{mc}{8\pi^2 e^2 \nu(v'v'')} \frac{g_u}{g_l} A_{v'v''}.$$

The intensities in emission are given by

$$\begin{aligned}
 I_{v',v''} &= N_{v'} h c \nu(v',v'') A_{v',v''} \\
 &= N_{v'} \frac{64}{3} \pi^4 c \frac{\nu^4(v',v'')}{g_u} R_e^2(\tilde{r}) q(v',v''),
 \end{aligned}$$

when expressed in energy per unit time, and  $N_{v'}$  is the number of molecules in level  $v'$ . Since the variation of  $R_e^2(\tilde{r})$  is small in comparison to  $q(v',v'')$ ,<sup>17</sup> one may use  $q(v',v'') \cdot \nu^4(v',v'')$  in estimating intensity distributions of bands in a system.

References

1. R. W. Wood, Phil. Mag. 10, 408 (1905).
2. A. C. G. Mitchell and M. W. Zemansky, "Resonance Radiation and Excited Atoms," University Press, Cambridge, 1961.
3. C. F. Meyer, Phys. Rev. 10, 91 (1917).
4. R. S. Becker, "Theory and Interpretation of Fluorescence and Phosphorescence," John Wiley and Sons, New York, 1969.
5. G. Herzberg, "Electronic Spectra and Electronic Structure of Polyatomic Molecules," Vol. III, D. Van Nostrand, Princeton, 1966.
6. D. L. Judge, A. L. Morse and G. L. Weissler, "Proc. VI Int. Conf. on Ionization Phenomena in Gases," Vol. III, page 373, Paris, 1963.
7. D. L. Judge and G. L. Weissler, J. Chem. Phys. 48, 4590 (1968).
8. D. L. Judge, G. S. Bloom, and A. L. Morse; Can. J. Phys. 47, 489 (1969).
9. K. H. Becker and K. H. Welge, Z. Naturforschg. 20a, 1692 (1965).
10. H. Okabe, J. Chem. Phys. 47, 101 (1967).
11. T. Carrington, J. Chem. Phys. 41, 2012 (1964).
12. R. A. Young, G. Black, and T. G. Slanger, J. Chem. Phys. 48, 2067 (1968).
13. A. B. Callear and I. W. M. Smith, Disc. Faraday Soc. 37, 96 (1964).

14. W. L. Weiss, M. W. Smith, and B. M. Glennon, "Atomic Transition Probabilities," Vol. I., Supt. of Documents, Washington, 1966.
15. M. Born and J. Oppenheimer, Ann. Physik 84, 457 (1927).
16. H. Honl and F. London, Z. Physik 33, 803 (1925); Ann. d. Phys., 273 (1925).
17. D. R. Bates, Monthly Not. Roy. Astron. Soc. 112, 614 (1952).
18. R. W. Nicholls, Ann. de Geophys., 20, 144 (1964).
19. R. J. Spindler, J. Q. S. R. T. 5, 165 (1962).
20. J. B. Coon, R. E. DeWames, and C. M. Loyd, J. Mol. Spectry 8, 285 (1962).
21. R. W. Nicholls and A. L. Stewart, "Atomic and Molecular Processes," p. 47, Academic Press, N. Y. (1962).
22. D. C. Jain and R. C. Sahni, Trans. Fara. Soc. 64, 3169 (1968).
23. R. W. Nicholls, J. Res. N. B. S., 68A, 535 (1964).
24. P. A. Frazer, Canadian J. Phys. 32, 515 (1954).

### 3.3 Experimental Details

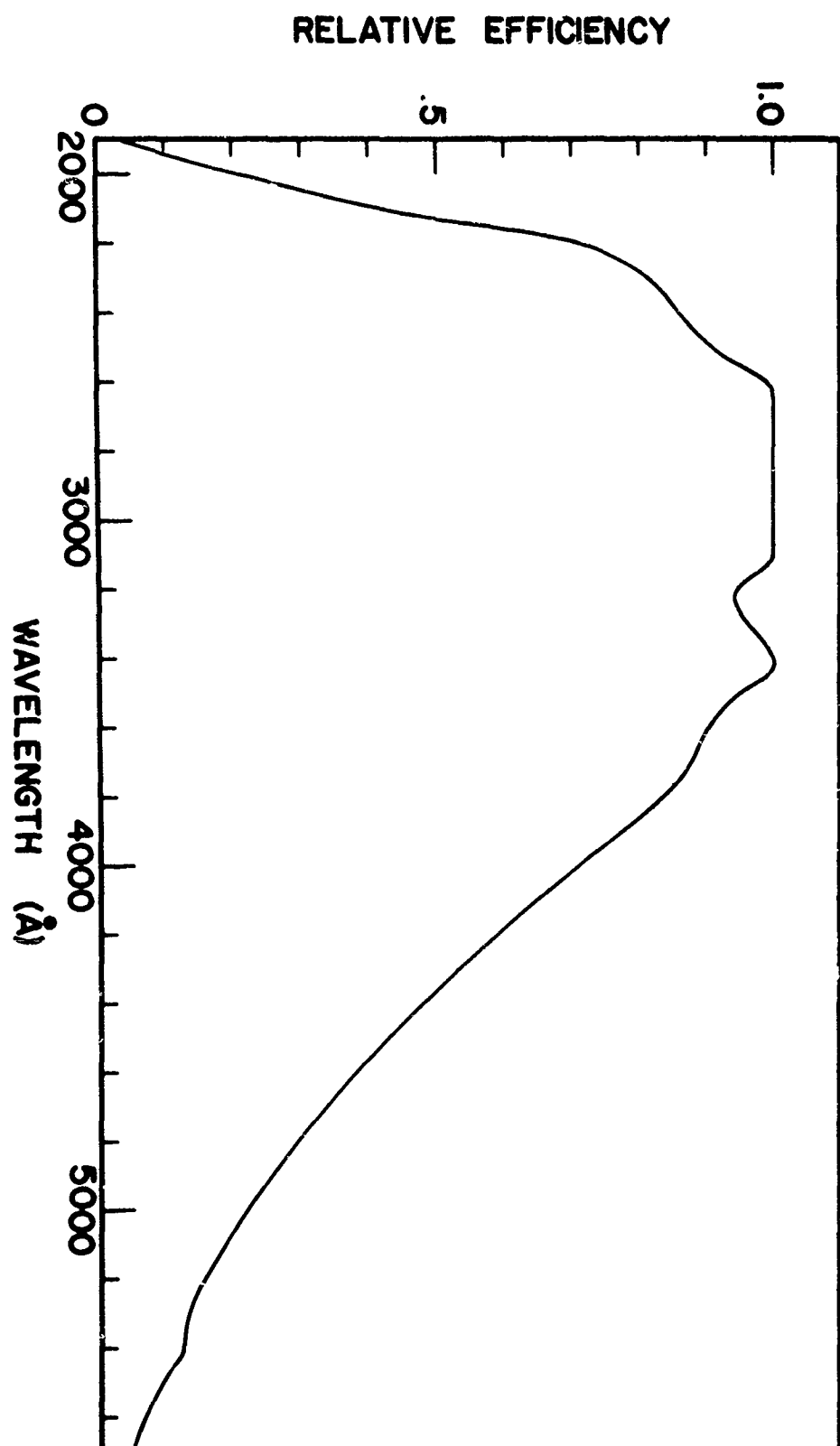
In our fluorescence study, a windowless hydrogen discharge tube operating at 0.35 amp dc with about 800 V across the tube was used. The experiments were performed with a McPherson 1-m vacuum monochromator. The experimental chamber was placed behind the exit slit of the monochromator, and LiF windows (1 mm x 25 mm diameter) was used to seal the chamber. The experimental chamber was connected to a gas-handling system, through which various gases can be introduced or pumped out from the chamber. A McLeod gauge, Hg and oil manometer, and CEC and MKS capacitor type pressure gauges were employed in measuring the pressure of the sample gas. The transmitted light was detected by a sodium salicylate coated glass mounted behind the experimental cell and an EMI - 9514S photomultiplier tube placed in air behind the plate. The phosphor converted the transmitted ultraviolet radiation into visible light, which was detected by the photomultiplier tube. The quantum efficiency of sodium salicylate was assumed to be constant over the region 500 to 2500 Å.<sup>1</sup>

The fluorescence was observed at right angles to the incident beam. In some experiments, the fluorescence was observed at 135°. The sodium salicylate coated photomultiplier was used to observe the resonance emission. while the uncoated quartz window was employed for total fluorescence measurements. A Suprasil quartz window was used to isolate the chamber from

the atmosphere. A 0.5 m Bausch and Lomb monochromator was placed behind this window to disperse the fluorescent radiation. The B and L monochromator utilizes a 1200 l/mm grating in an Ebert type mount. The slit width was approximately 1 mm. We placed an EMI - 6255S photomultiplier tube cooled with boiling liquid nitrogen behind the exit slit to detect the dispersed radiation. Commercial photon-counting equipment was used and the dark background count was about 10 counts per second. In order to compare intensities of the emission lines, a relative response curve of the B and L monochromator and EMI detector system was obtained with the use of a quartz-iodine lamp<sup>2,3</sup> for the 2500 to 6000 Å region and the H<sub>2</sub> light source and McPherson monochromator for the 1800 to 3000 Å. This curve is shown in Fig. 1.

In total fluorescence measurements, the McPherson monochromator could scan from 1050 to 2000 Å with the detectors viewing the emission. The dispersed fluorescence measurements were made with the McPherson monochromator (bandwidth 10 Å) set on an excitation wavelength while the B and L monochromator scanned from 1800 to 6000 Å. Measurements were made under static gas pressures and flow conditions. The steady flow was necessary to remove the dissociated products.

The gases were obtained from the Matheson Company in pyrex bulbs (assayed reagent) and in compressed gas cylinders (various grades). Some gases were further purified and stored in pyrex bulbs. Due to the large size of the fluorescence chamber, the



34  
Fig. 1 (Sec. 3.3). Relative response curve of B & L monochromator and detector system.

compressed cylinder gases were used without further purification.

Gases which showed signs of impurities were rejected.

#### References

1. K. Watanabe and E. C. Y. Inn, J. Opt. Soc. Am. 43, 32 (1953).
2. R. Stair, W. E. Schneider, J. K. Jackson, Applied Optics 2, 1151 (1963).
3. R. M. St. John, "Method of Experimental Physics" Vol. 8, p. 27, Academic Press, New York, 1969.



### 3.4 Relating Measured Emissions to Franck-Condon Factors

Molecular band emission intensities for electric dipole transitions are given by

$$I(v'v'') = N_{v'} \frac{64}{3} \pi^4 c \frac{\nu^4(v'v'')}{g_u} R_e^2(\bar{r}) q(v'v'')$$

$$= K_1 N_{v'} \nu^4(v'v'') q(v'v''),$$

where  $K_1$  is a constant. If the intensity of emission can be expressed in terms of  $i(v'v'')$  in counts per second (the peak photomultiplier output corresponding to a fluorescence transition from some vibrational level  $v'$  to a lower level  $v''$ ) and  $\eta(v'v'')$  the relative efficiency of the fluorescence analyzing system, we may write

$$I(v'v'') = K_2 i(v'v'') \nu(v'v'')/\eta(v'v''),$$

and

$$N_{v'} = K_3 \sum_{v''} i(v'v'')/\eta(v'v''),$$

where  $K_2$  and  $K_3$  are constants of proportionality. Solving the equations for  $q(v'v'')$  in terms of the measured values, we have

$$q(v'v'') = \frac{K_2 K_4 i(v'v'')/\eta(v'v'')}{K_1 K_3 \sum_{v''} i(v'v'')/\eta(v'v'')} \cdot \frac{1}{\nu^3(v'v'')},$$

where  $K_4$  is the normalizing factor such that  $\sum_{v''} q(v'v'') = 1$ .

The band emission data were obtained with low gas pressures so that the absorption of the emitted radiation could be neglected.

### 3.5 Carbon Monoxide (CO)

#### Introduction

The absorption and emission spectra of CO have been studied by many investigators. Krupenie<sup>1</sup> has made a detailed summary of the results prior to 1966. There are several strong transitions such as  $A^1\Pi - X^1\Sigma^+$ ,  $B^1\Sigma^+ - X^1\Sigma^+$ ,  $C^1\Sigma^+ - X^1\Sigma^+$ , and  $E^1\Pi - X^1\Sigma^+$ , which lie in the region 1000 to 2000 Å. In this same region of the spectrum the transitions of six weaker forbidden systems have been observed.<sup>2</sup> The emission spectrum has been of interest since the 4th positive system ( $A^1\Pi - X^1\Sigma^+$ ) has been identified in the solar spectrum.<sup>3,4</sup> The other emission system studied in detail are the Angstrom bands ( $B^1\Sigma^+ - A^1\Pi$ ) and the Herzberg bands ( $C^1\Sigma^+ - A^1\Pi$ ).<sup>1</sup> The absorption cross sections were measured with 1Å resolution by Watanabe, *et al.*,<sup>5</sup> and more recently, by Myer and Samson<sup>6</sup> with 0.25 Å resolution. Experimental scattering cross sections in the 1000 to 2000 Å region were reported by Marmo.<sup>7</sup>

Radiative lifetime measurements on several A - B, B - C, and C - X transitions have been made by Hesser and Dressler.<sup>8,9</sup> Franck-Condon factors have been calculated by Nicholls and co-workers.<sup>10,11</sup> Fluorescence of CO induced by radiation from rare gas resonance light sources have been studied by Becker and Welge,<sup>12</sup> and Slanger and Black.<sup>13,14</sup> Emission from the  $A^1\Pi$ ,  $a^1\Sigma^+$ ,  $d^3\Delta$ , and  $e^3\Sigma^-$  states were observed. Three triplet state

transitions to the  $a^3\Pi$  state were observed in the 5000 to 6000 Å region. In the present investigation the fluorescence due to the Fourth Positive, Angstrom, and Herzberg bands were studied in the region 2000 to 5200 Å. Franck-Condon factors were measured and compared with theoretical values.

#### Discussion

The excitation spectrum of CO was obtained with about 1 Å resolution in the region 1050 to 2000 Å. A sodium salicylate coated disk was placed in front of the photomultiplier mounted normal to the excitation radiation to view the undispersed uv fluorescent radiation and the disk was removed to view the fluorescence greater than 3000 Å. The excitation spectrum showed the A - X, B - X, C - X, and E - X transitions to be intense while the triplet states  $a'$ , e, and d were weak as expected. In many cases the triplet states overlapped the strong singlet transitions.

The dispersed fluorescence spectrum of A  $\rightarrow$  X, (5,  $v''$ ) and (6,  $v''$ ) were obtained. The Angstrom band (0,  $v''$ ), and Herzberg band (0,  $v''$ ) were also obtained. Figs. 1, 2, 3, and 4 show the fluorescence spectrum as a function of wavelength. The experimental Franck-Condon factors are compared with the theoretical values in Tables I, II, and III. The results are in good agreement with the theory.<sup>10,11</sup>

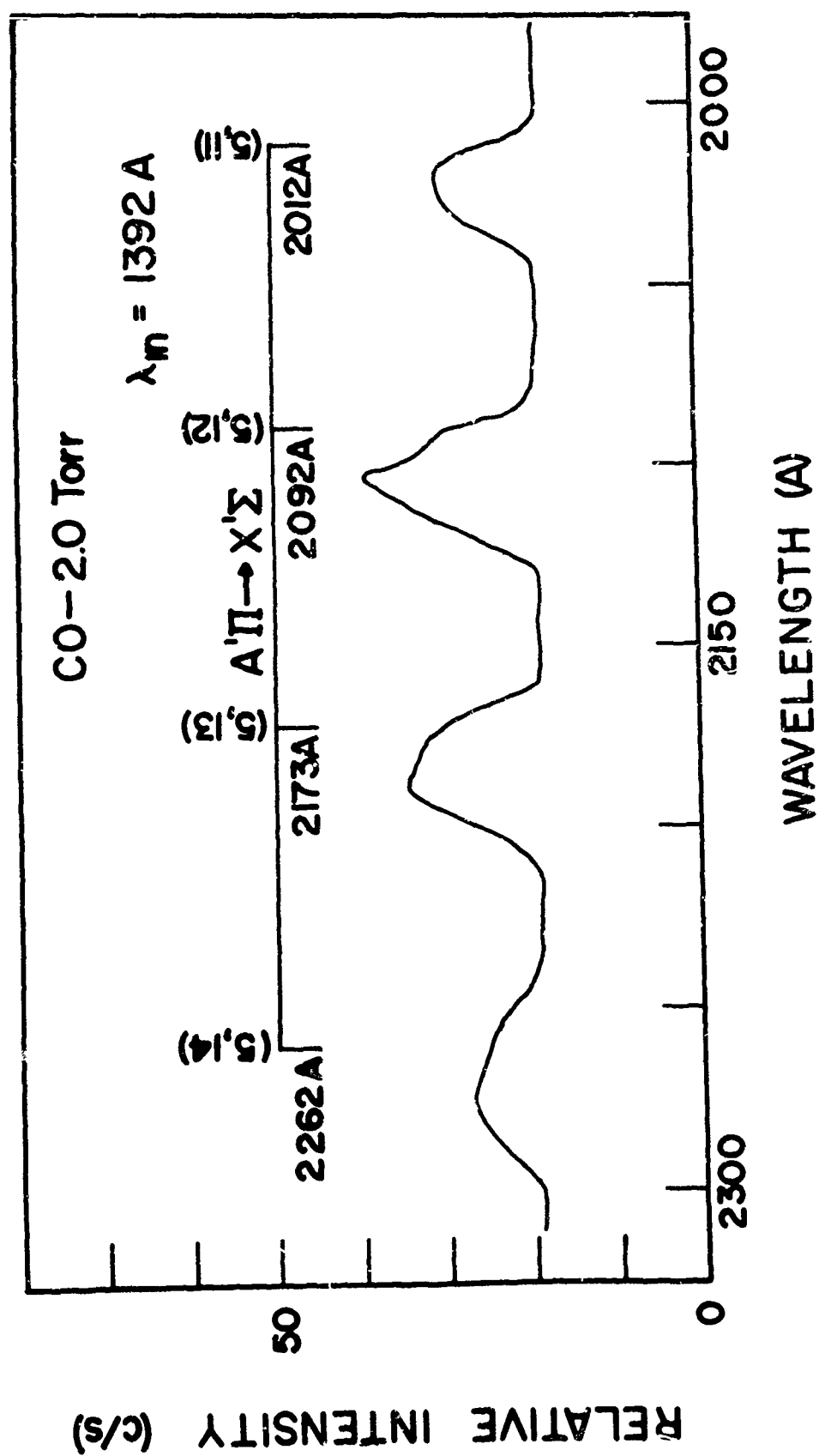


Fig. 1 (Sec. 3.5). Fluorescence of CO - 4th positive bands.

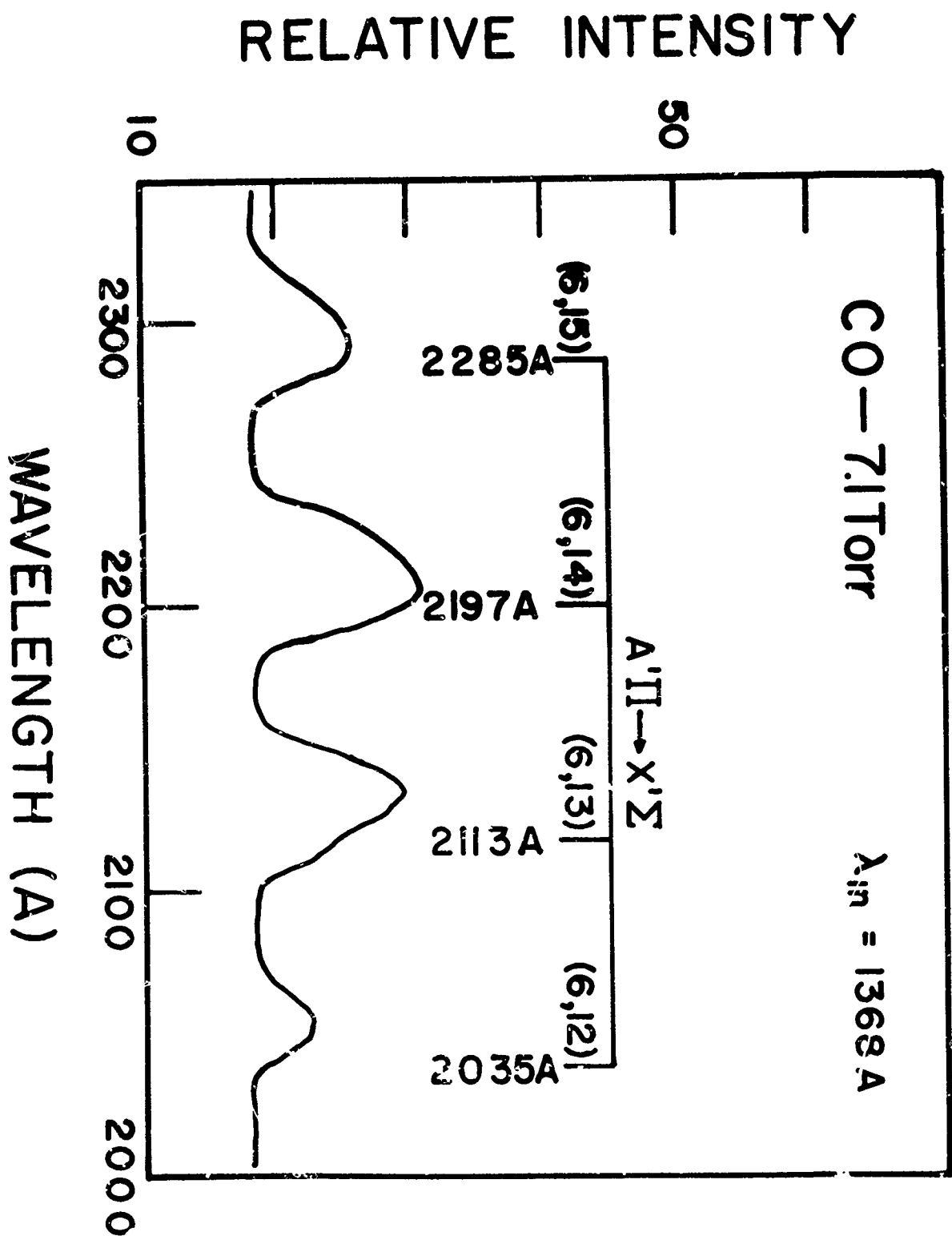


Fig. 2 (Sec. 3.5). Fluorescence of CO — 4th positive bands.

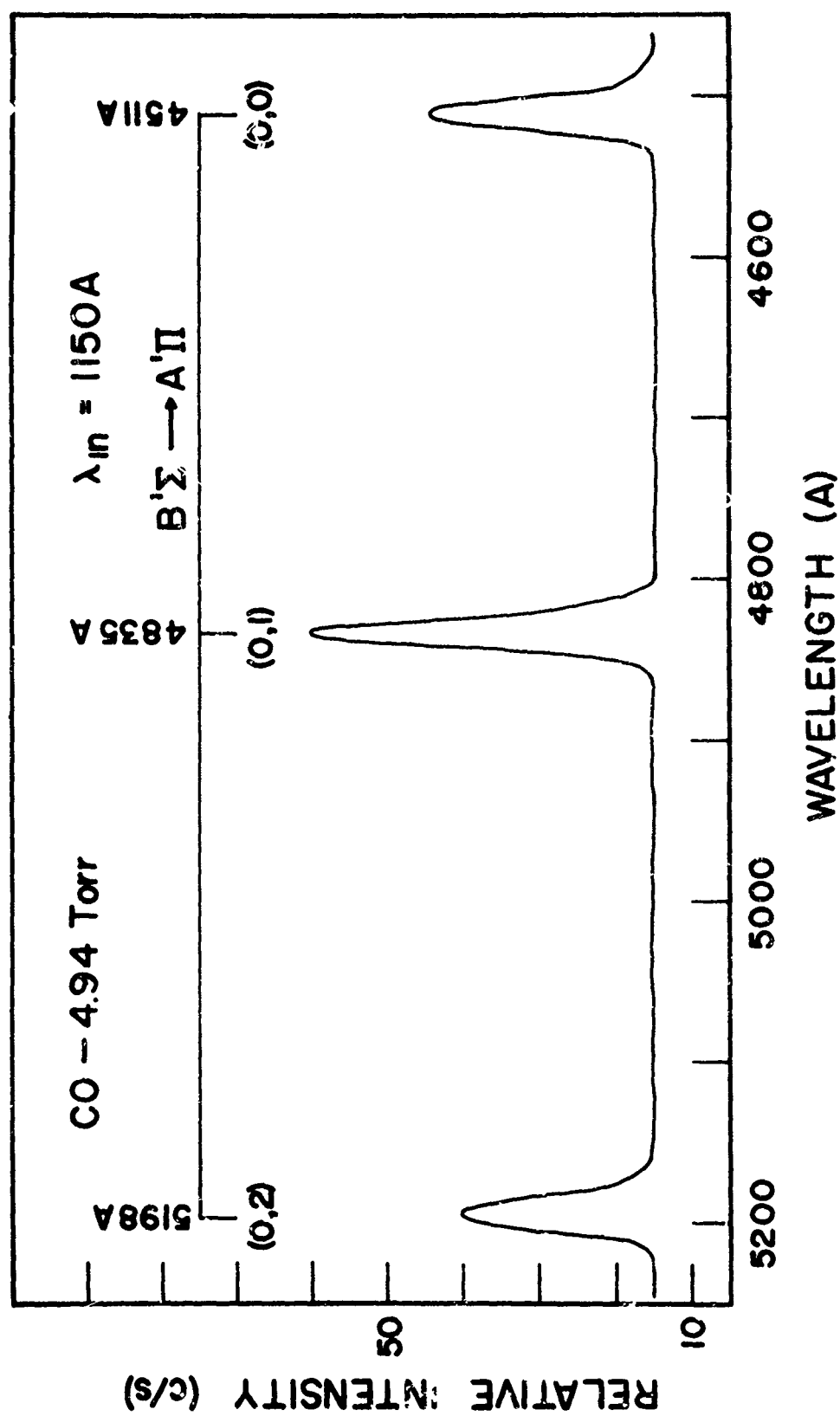


Fig. 3 (Sec. 3.5). Fluorescence of CO - Angstrom bands.

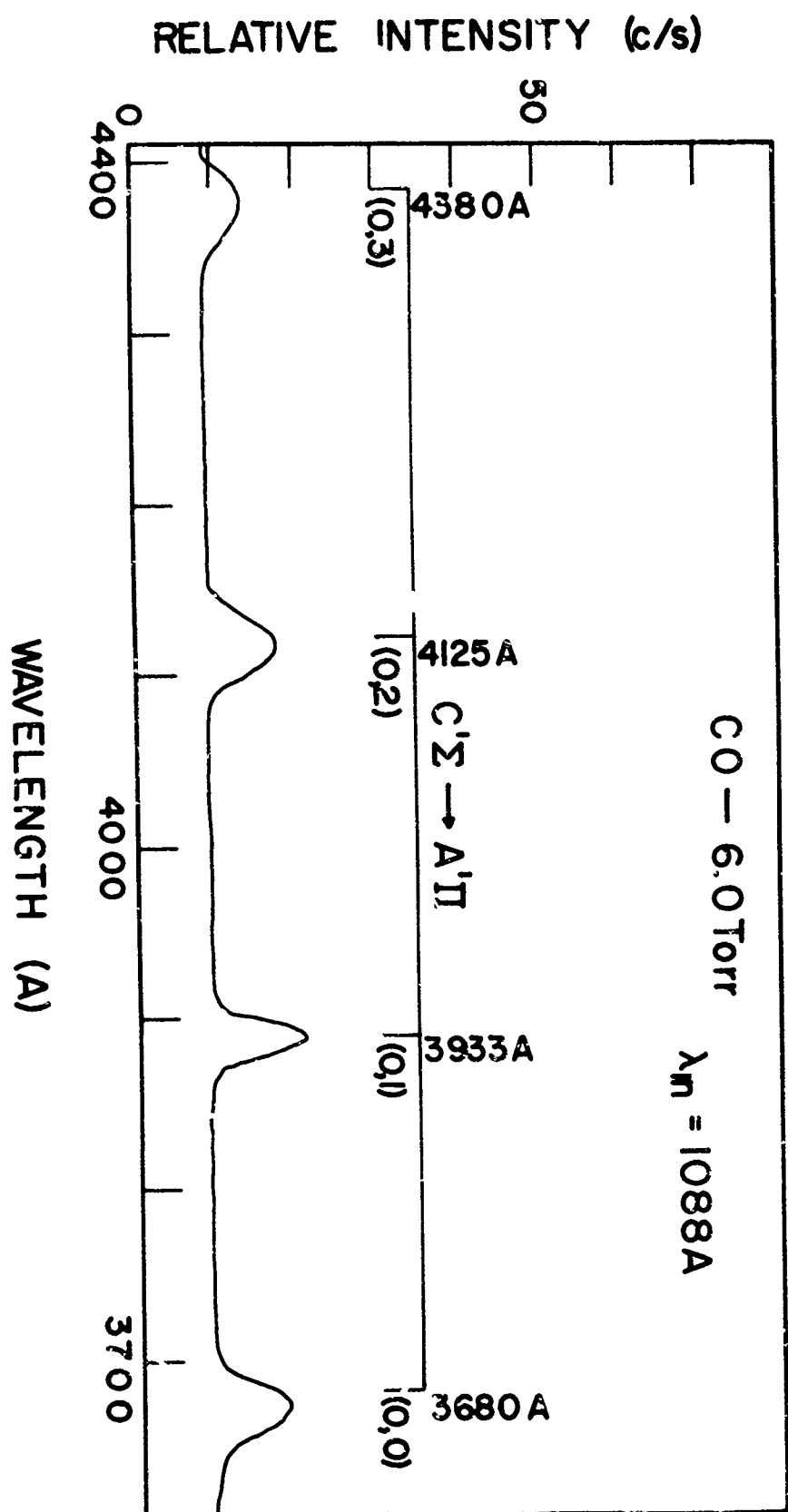


Fig. 4 (Sec. 3.5). Fluorescence of CO - Herzberg bands.

Table I. Comparison of Franck-Condon factors for  $A^1\Pi \rightarrow X^1\Sigma^+$  transitions of CO.

$v', v''$	$q_{v', v''}$ (Exp)	$q_{v', v''}$ (Theory) <sup>a</sup>
5, 11	$0.35 \pm 0.14$	0.27
5, 12	$0.36 \pm 0.12$	0.36
5, 13	$0.19 \pm 0.06$	0.25
5, 14	$0.10 \pm 0.04$	0.12
6, 12	$0.18 \pm 0.11$	0.11
6, 13	$0.36 \pm 0.15$	0.33
6, 14	$0.30 \pm 0.11$	0.35
6, 15	$0.16 \pm 0.08$	0.21

a. reference 11.



Table II. Comparison of Franck-Condon factors for the Angstrom bands ( $B^1\Sigma^+ \rightarrow A^1\Pi$ ) of CO.

$v'v''$	$q_{v'v''}$ (Exp.)	$q_{v'v''}$ (Theory) <sup>b</sup>
0, 0	$0.14 \pm 0.03$	0.18
0, 1	$0.38 \pm 0.08$	0.39
0, 2	$0.48 \pm 0.12$	0.44

Table III. Experimental Franck-Condon factors for the Herzberg bands ( $C^1\Sigma^+ \rightarrow A^1\Pi$ ) of CO.

$v'v''$	$q_{v'v''}$ (Exp.)
0, 0	$0.17 \pm 0.07$
0, 1	$0.27 \pm 0.09$
0, 2	$0.26 \pm 0.10$
0, 3	$0.30 \pm 0.20$

b. reference 10.

## References

45

1. P. H. Krupenie, NBS, National Standard Reference Data Series, NBS - 5 (1966).
2. J. D. Simmons, A. M. Bass, S. G. Tilford; Astrophysics J. 155, 345 (1969).
3. L. Goldberg, W. H. Parkinson, and E. M. Reeves, Astrophysics J. 141, 1293 (1965).
4. J. R. Porter, S. G. Tilford, and K. G. Widing, Astrophys. J. 147, 172 (1967).
5. K. Watanabe, M. Zelikoff and E. C. Y. Inn, Geophys. Res. Papers No. 21, AFCRL (1953).
6. J. N. Meyer and J. A. R. Samson, J. C. P. 52, 266 (1970).
7. F. F. Marmo, GCA Report TR-68-7-N (1968).
8. J. E. Hesser and K. Dressler, Astrophysical J. 142, 329 (1965).
9. J. E. Hesser and K. Dressler, J. C. P. 45, 3149 (1966).
10. R. W. Nicholls, P. A. Frazer, W. R. Jarman and R. P. McEachran, Astrophys. J. 131, 399 (1960).
11. R. W. Nicholls, J. Q. R. S. T. 2, 433 (1962).
12. K. H. Becker and K. H. Welge, Z. Naturforsch. 20a, 1692 (1965).
13. T. G. Slanger, J. C. P. 48, 586 (1968).
14. T. G. Slanger and G. Black, J. C. P. 51, 4534 (1969).

3.6 Ammonia (NH<sub>3</sub>)

## Introduction

The absorption spectrum of ammonia in the vacuum ultraviolet has been extensively studied. Herzberg<sup>1</sup> has reviewed the investigations prior to 1966. Absorption and photoionization coefficients were measured by Watanabe and Sood<sup>2,3</sup> in the spectral region 600 to 2200 Å. In the region 1050 to 2200 Å, there appear to be at least three continua underlying the numerous bands. McNesby and Okabe<sup>4</sup> have reviewed the investigations on the photodissociation processes by means of conventional product analysis, flash absorption spectroscopy, fluorescence, and photoionization. The emission observed when ammonia was irradiated with 1050 to 1700 Å radiation was primarily due to the photodissociated products of ammonia, e.g. NH<sub>2</sub> and NH.<sup>5-7</sup> Okabe and Lenzi<sup>7</sup> by use of filters obtained relative fluorescence curves of NH<sub>2</sub>  $\tilde{A}A_1 \rightarrow \tilde{X}^2B_1$ , and NH  $c^1\Pi \rightarrow a^1\Delta$  emission. The threshold energy for the production of NH ( $c^1\Pi$ ) was obtained and from that the energy level separation of the NH ( $a^1\Delta$ ) state with respect to the ground state NH ( $X^3\Sigma^-$ ) was determined to be  $\leq 1.6 \pm 0.1$  eV.<sup>7</sup> Foner and Hudson<sup>8</sup> obtained values ranging from 1.6 to 2.2 eV from appearance potential measurements, while Hurley<sup>9</sup> calculated  $1.76 \pm 0.2$  eV using orbitals with an interatomic correction and Huo<sup>10</sup> obtained 1.83 eV by means of single configuration SCF calculations.

The purpose of this study was to disperse the fluorescent

radiation and to identify the photodissociated products, and also to determine the separation of the  $\text{NH } a^1\Delta - X^3\Sigma^-$  energy levels.

#### Discussion

The experimental traces are shown in Fig. 1. The upper curve shows the intensity distribution of the  $\text{H}_2$  emission lamp in the region 900 to 1700 Å. The middle trace shows the excitation spectrum with  $\text{NH } c^1\Pi \rightarrow a^1\Delta$  emission, since the Bausch and Lomb monochromator was set at 3240 Å. The lower trace was taken with the Bausch and Lomb monochromator set at central image and a 3700 Å cutoff filter placed in front of the entrance slit. The  $\text{NH } c^1\Pi \rightarrow a^1\Delta$  emission trace shows the threshold at about  $1245 \pm 10$  Å which disagrees with the value obtained by Okabe and Lenzi,<sup>7</sup> i.e.  $1325 \pm 7$  Å. The ratio of the fluorescence intensity to the incident intensity ( $I_f/I_o$ ) are in good agreement when normalized to the curve published by Okabe and Lenzi<sup>7</sup> in the region 1100 to 1230 Å. Fig. 2 shows the photodissociation point. The photodissociation tail is similar to the photoionization yield tail<sup>2</sup> where they tend to follow a Boltzmann distribution for the population of higher vibrational levels of the ground state. Our results beyond 1230 Å shows a definite threshold while the curve of Okabe and Lenzi<sup>7</sup> remains constant to their threshold of about 1325 Å. This may be due to their use of a broad band filter 2200 to 4200 Å instead of a monochromator.  $\text{NH}_2 \ \tilde{A}^2A_1 \rightarrow \tilde{X}^2B_1$  emission (3800 to 4200 Å) was probably excited with photon energy

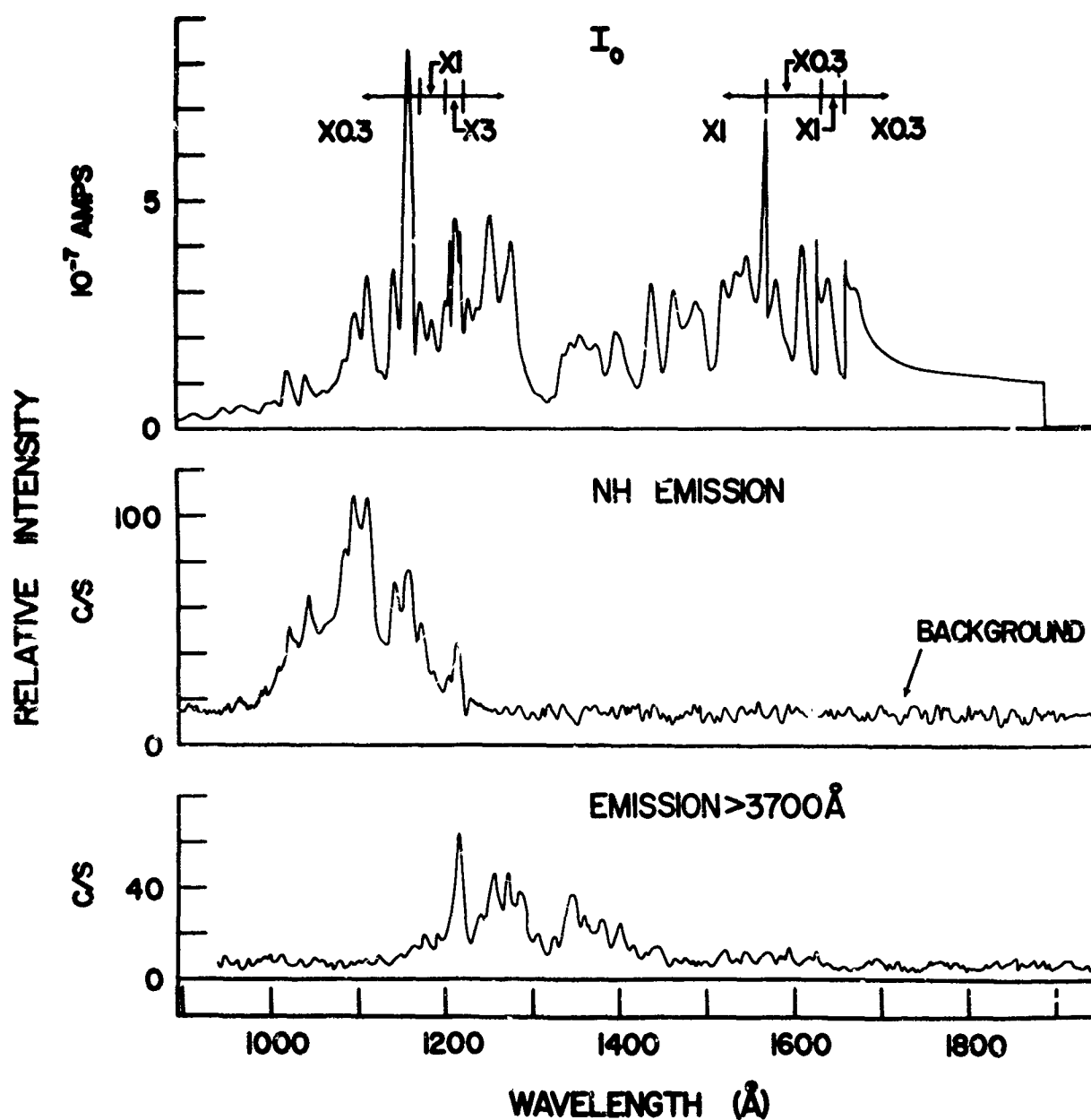


Fig. 1 (Sec. 3.6). Hydrogen light source intensity distribution (upper curve). Excitation spectrum for NH emission, 0.10 Torr  $\text{NH}_3$  (middle curve). Excitation spectrum for emission  $> 3700 \text{ Å}$ , 0.10 Torr  $\text{NH}_3$  (lower curve).

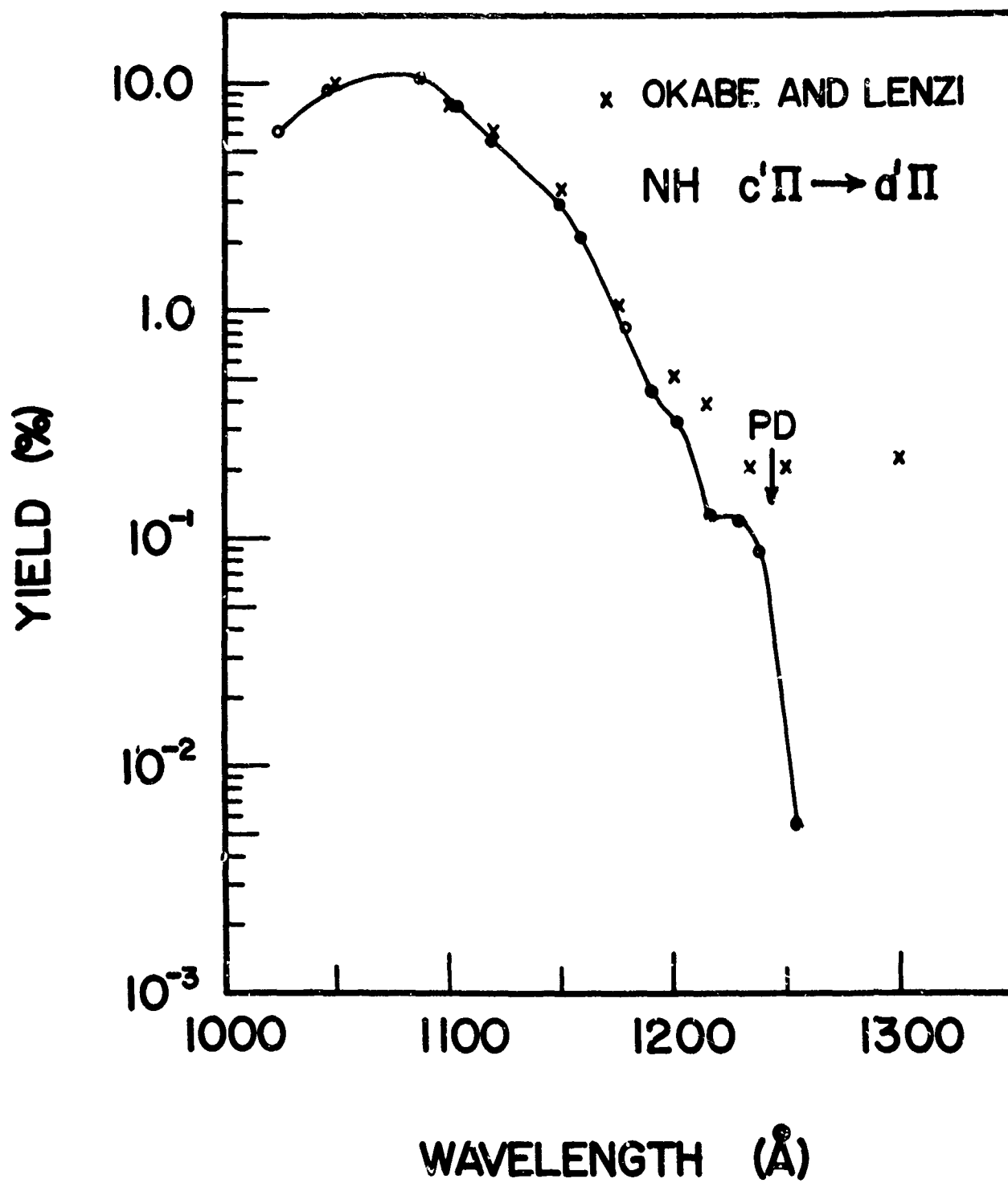


Fig. 2 (Sec. 3.6). NH fluorescence yield curve.

greater than 9.35 eV (1325 Å), since the threshold for  $\text{NH}_3 + h\nu \longrightarrow \text{NH}_2(\tilde{\text{A}}^2\text{A}) + \text{H}(^2\text{S})$  is 5.70 eV,<sup>7</sup> and the additional energy of 3.7 eV may populate higher levels of  $\tilde{\text{A}}^2\text{A}$ . Although Becker and Welge<sup>6</sup> reported weak  $\text{NH } c^1\Pi \longrightarrow a^1\Delta$  emission excited by the weak xenon resonance line at 1295 Å, their results may be affected by impurity emission lines less than 1250 Å since the light source radiation was undispersed.

The threshold energy for the appearance of the  $\text{NH } c^1\Pi \longrightarrow a^1\Delta$  emission can be used to calculate the energy separation of the  $a^1\Delta$  state from the  $X^3\Sigma^-$  ground state of  $\text{NH}$ . Following the method of Okabe and Lenzi<sup>7</sup> we obtain  $2.2 \pm 0.1$  eV as compared to their value of  $1.6 \pm 0.1$  eV. Both results are in agreement with the appearance potential values<sup>8</sup> and theoretical values.<sup>9,10</sup> The absorption curve of Watanabe and Sood<sup>2,3</sup> show an underlying continuum from the  $\text{LiF}$  cutoff to about 1260 Å, 1260 to 1550 Å, and 1550 to 2200 Å. The first one up to 1260 Å appears to be correlated with  $\text{NH } c^1\Pi$  production.

The excitation spectrum obtained with an EMI - 6255S photomultiplier showed the  $\text{NH}_3 \tilde{\text{B}}^1\text{E}'' - \tilde{\text{X}}^1\text{A}$  bands  $v' = 2$  to 8, and  $\tilde{\text{D}}^1\text{A}_2'' - \tilde{\text{X}}^1\text{A}$  bands  $v' = 0$  to 11 fluorescing. This is in agreement with Okabe and Lenzi who suggested that all discrete transitions as well as the continuum dissociates into  $\text{NH}_2 \tilde{\text{A}}^2\text{A}_1 + \text{H}(^2\text{S})$  in the region 1650 to 1200 Å.

References

1. G. Herzberg, "Molecular Spectra and Molecular Structure",  
vol. 3, p. 580, 609, D. Van Nostrand, Princeton, 1966.
2. K. Watanabe, J. Chem. Phys. 22, 1564 (1954).
3. K. Watanabe and S. P. Sood, Sci. Light (Tokyo) 14, 36 (1965).
4. J. R. McNesby and H. Okabe, Adv. Photochem. 3, 157 (1964).
5. H. Neuimin and A. Terenin, Acta Physicochemica USSR 5,  
456 (1936).
6. K. H. Becker and K. H. Welge, Z. Naturforsch. 18a, 600  
(1963).
7. H. Okabe and M. Lenzi, J. Chem. Phys. 47, 5241 (1967).
8. F. N. Foner and R. L. Hudson, J. Chem. Phys. 45, 40 (1966).
9. A. C. Hurley, Proc. Roy. Soc. (Lond.) A249, 402 (1959).
10. W. M. Huo, J. Chem. Phys. 49, 1482 (1968).



### 3.7 Nitric Oxide (NO)

#### Introduction

The absorption and emission spectra of NO have been studied in detail. A review of the spectroscopy and the role of NO in photochemistry was published in 1968 by Heiklen and Cohen.<sup>1</sup> Recent investigations have been made by Miescher and co-workers.<sup>2-6</sup> The electronic absorption spectrum of NO starts below 2300 Å and extends into the VUV. Gilmore<sup>7</sup> has published potential energy curves for most of the electronic states and Fig. 1 shows some of the curves. Transitions between the ground electronic state  $X^2\Pi$  and the  $A^2\Sigma^+$ ,  $B^2\Pi$ ,  $C^2\Pi$ ,  $D^2\Sigma^+$ ,  $E^2\Sigma^+$ , and  $B'^2\Delta$  states are referred to as  $\gamma$ ,  $\beta$ ,  $\delta$ ,  $\epsilon$ ,  $\gamma'$  and  $\beta'$  bands, respectively. Emission has never been observed in the  $\beta$  system for  $v' > 7$ . In the  $\delta$  system no emission has been detected for  $v' > 0$  and even the zero level predissociates. The results are consistent with the dissociation energy of 6.50 eV.<sup>3</sup> Emission from other upper states to the ground state have also been observed, i.e.,  $F^2\Delta - X^2\Pi$ , and  $N^2\Delta - X^2\Pi$ .<sup>8</sup> Nearly all  $^2\Sigma$  and  $^2\Pi$  levels above the dissociation limit of the ground state atoms are missing because of predissociation by the repulsive  $A'^2\Sigma^+$  state, so that the  $^2\Delta$  levels are almost the only ones leading to emission at higher energies.<sup>8</sup> In our present study the levels populated are listed in Table I with the allowed transitions.

Recently, fluorescence studies of NO excited by VUV mono-

chromatic radiation were made by Callear and Smith,<sup>9</sup> and Young, et al.<sup>10</sup> The former used a xenon continuum light source above 1800 Å, while the latter used Hg and rare gas resonance light sources which emitted radiation of wavelengths 1849, 1470, 1165 and 1236, and 1048 and 1067 Å, respectively. Okabe<sup>11</sup> used a broad filter (2200 to 4100 Å bandwidth) detector and an H<sub>2</sub> discharge light source to observe the excitation spectrum of NO in the region 2000 to 1050 Å. The intensity of the emission bands can be related to oscillator strengths and Franck-Condon factors. Wray<sup>12</sup> has reported oscillator strengths for nine transitions between Rydberg states in the near infrared region, and Ory<sup>13</sup> reported on oscillator strengths for γ, β, δ, and ε systems. Nicholls<sup>14</sup> has published Franck-Condon factors for most of the allowed transitions. Spindler, et al.,<sup>15</sup> have used the RKR type potentials to obtain Franck-Condon factors for the γ system which was in good agreement with the results of Nicholls who used Morse type potentials.

The purpose of this investigation was to investigate the fluorescence of NO excited by monochromatic radiation in the region 2300 to 1400 Å.

#### Results and Discussion

The fluorescence spectrum of NO in the region 1680 to 1430 Å is shown in Fig. 2. This was obtained with the EMI - 6255S photomultiplier placed at right angles to the excitation radia-

tion ( $1 \text{ \AA}$  bandwidth). The photon detector was sensitive to fluorescence in the region 1900 to  $6500 \text{ \AA}$ . The ratio of fluorescent intensity to incident intensity was normalized to unity at  $1635 \text{ \AA}$ . The excitation spectra show many overlapping states. The H, H' states show weak emission in the visible. With excitation of wavelength  $1470 \text{ \AA}$  from our source, the emission was weak; however, Young, *et al*<sup>10</sup> observed  $H' \rightarrow A(2, 2)$ ,  $B' \rightarrow B(3, 0 + 5, 3 + 2, 0)$ ,  $E \rightarrow A(0, 0 + 1, 1 + 2, 2)$ ,  $O' \rightarrow C(0, 0)$ ,  $O' \rightarrow D(0, 0)$ ,  $N \rightarrow C(0, 0)$  and  $B' \rightarrow C(7, 0)$  transitions using a strong resonance lamp at  $1470 \text{ \AA}$ .

In order to have sufficient intensity to populate the NO upper states, the exit slit for exciting radiation was set for a bandwidth of  $10 \text{ \AA}$  while the Bausch and Lomb monochromator was adjusted for a bandwidth of  $18 \text{ \AA}$ . Figures 3, 4, 5 and 6 show typical fluorescence of NO excited by light of 1640, 1610, 1580 and  $1550 \text{ \AA}$ , respectively. Figure 2 shows that the excitation wavelengths corresponding to the depopulation of the B', D, E, and F states. Tables II, III, IV, and V show the transitions observed. The emission wavelengths listed are averaged because the excitation wavelength populated several upper states. The Franck-Condon factors  $q_{v',v''}$  calculated by Nicholls<sup>14</sup> indicate that  $B' \rightarrow X$  transitions to high vibrational number  $v'' > 6$  give rise to intense emission. Some  $q_{v',v''}$  for D, E, and F states were found to be comparable to  $B' \rightarrow X$  transitions. For Rydberg states (A, C, D, E, F, K) the shape of the potential energy

curves are almost identical, and the internuclear separation for the various states are very nearly equal (see Fig. 1). Hence, the  $q_{v',v''}$  are very nearly unity for  $\Delta v = 0$  and should be quite small for  $\Delta v \neq 0$ , as shown by calculations for several Rydberg systems.<sup>14</sup> Visible and infrared systems arise from  $F \rightarrow C$ ,  $E \rightarrow A$ ,  $D \rightarrow A$ , and  $C \rightarrow A$  transitions, while  $A \rightarrow X$  is in the ultraviolet. Transitions involving the non-Rydberg  $B'$  state are  $B \rightarrow X$ ,  $B' \rightarrow B$ , and  $B' \rightarrow C$  (4, 1) and (7, 0). Since the  $C$  state predissociates there are no  $C \rightarrow A$ , and  $C \rightarrow X$  emission for  $v' > 0$ .

Some experimental  $q_{v',v''}$  are tabulated in Table VI. These bands were relatively free from overlap by other states. The  $B' \rightarrow X$  (1,  $v''$ ) results were obtained by neglecting the contribution of  $E \rightarrow X$  (0,  $v''$ ),  $v'' \geq 6$ , since the  $q_{0v''}$  of the  $\gamma'$  system were much smaller than the  $q_{1v''}$  of the  $\beta'$  system. Also, since the  $2\Delta$  states are not as strongly affected by predissociation of the  $2\Sigma^+$  and  $2\Pi$  states, the  $B'$  system should dominate.<sup>8</sup> The results are in good agreement with calculated values of Nicholls,<sup>14</sup> indicating the  $\gamma'$  band contribution is negligible. Most of the other systems were overlapped by  $A \rightarrow X$  and  $B \rightarrow X$  transitions because the upper states  $B'$ ,  $D$ ,  $E$ , and  $F$  cascade to the  $A$  and  $B$  levels by radiative decay. Due to our lack of resolution, quantitative  $q_{v',v''}$  were not obtained for many transitions. In Fig. 6, the  $A \rightarrow X$  (0,  $v''$ ) may be ascribed to the  $K^2\Pi$  ( $v = 0$ ) state cascading to the  $A^2\Sigma$  ( $v' = 0$ ) directly or via  $C$  ( $v = 0$ )

and D ( $v = 0$ ) states, although Huber<sup>16</sup> reported the absence of emission bands with K, M or S upper states due to weak predissociation. Wray<sup>12</sup> reported an experimental oscillator strength  $f < 0.08$  for  $K \rightarrow D$  emission, but he did not investigate the  $K \rightarrow A$ , and  $K \rightarrow C$  transitions. With our present experimental arrangement we were not able to investigate emission due to  $K \rightarrow A$  and  $E \rightarrow A$  because of the limited response of our analyzing system.

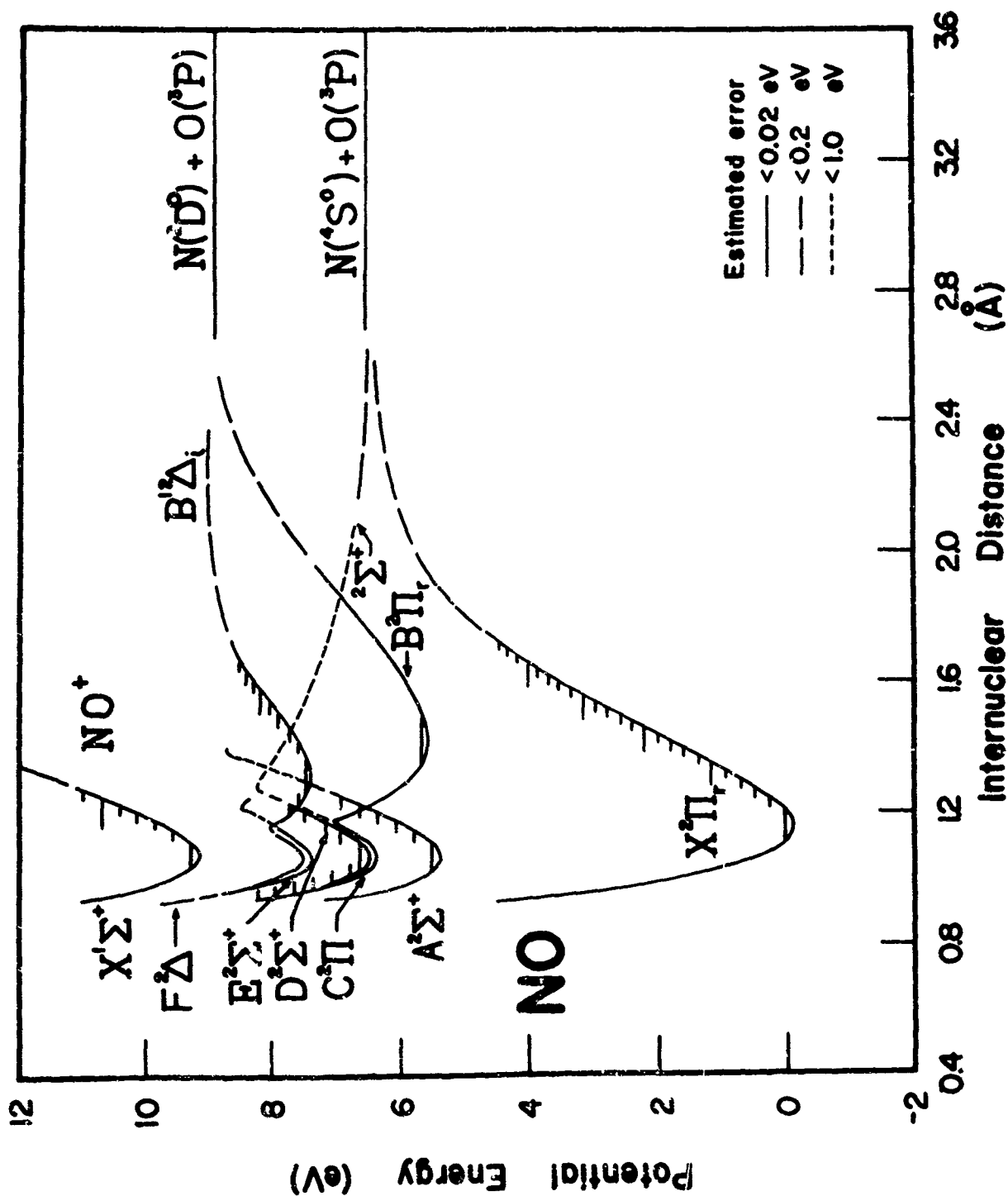
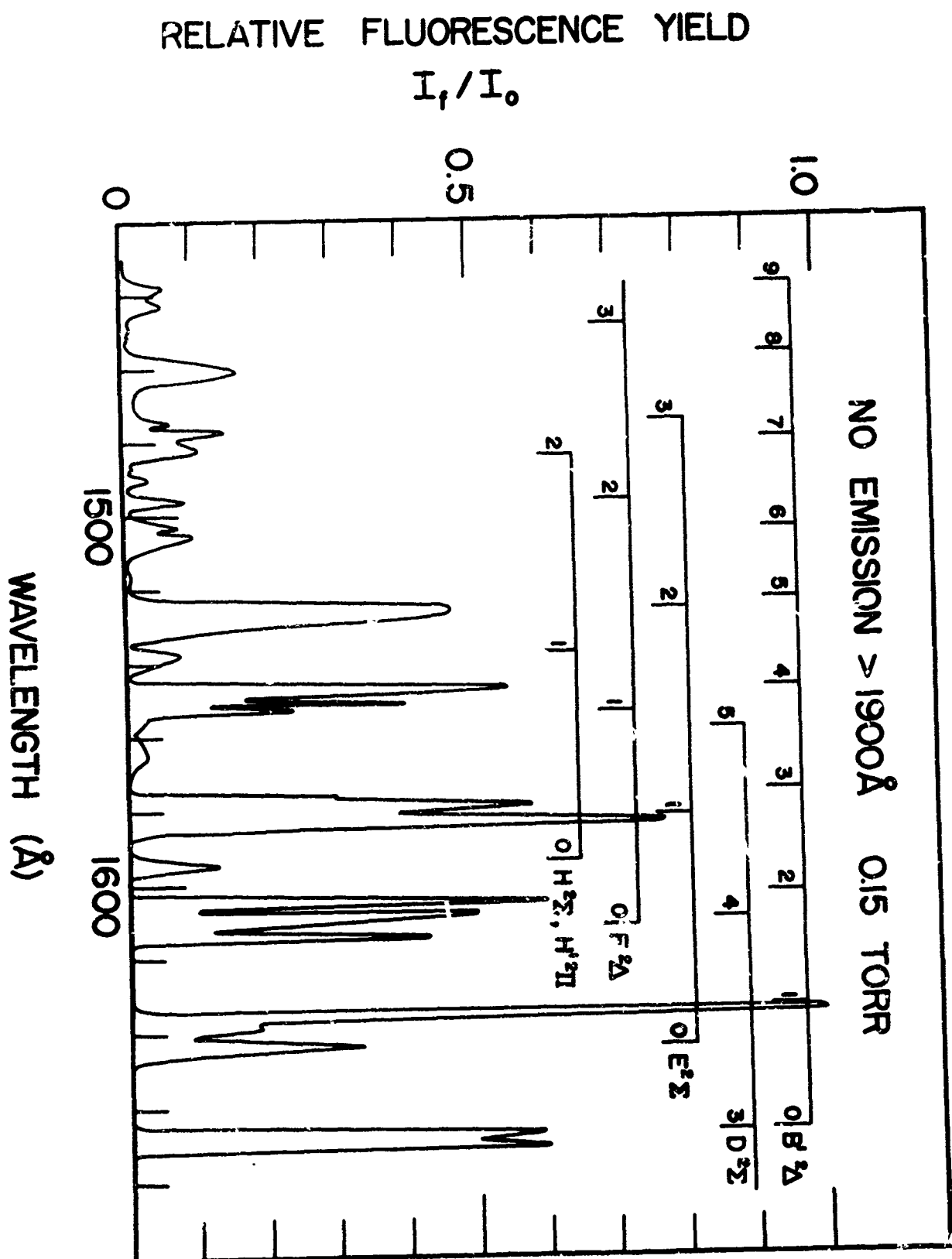


Fig. 1 (Sec. 3.7). Potential energy diagram of NO (F. R. Gilmore, J.Q.S.R.T. 5, 369 (1964)).

58  
Fig. 2 (Sec. 3.7). NO excitation spectrum for emission > 1900 Å.



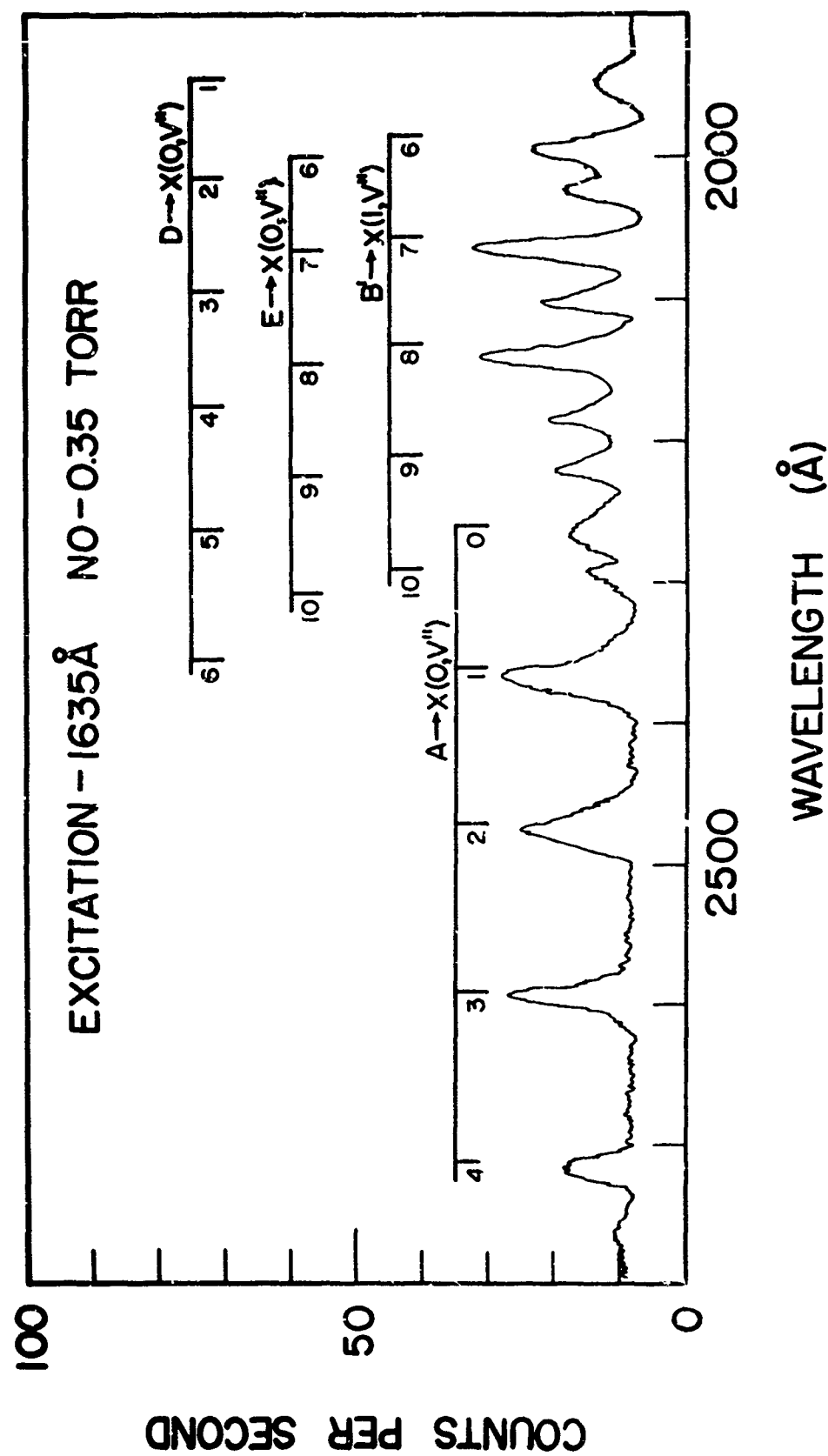


Fig. 3 (Sec. 3.7). NO fluorescence excited by 1635 Å.



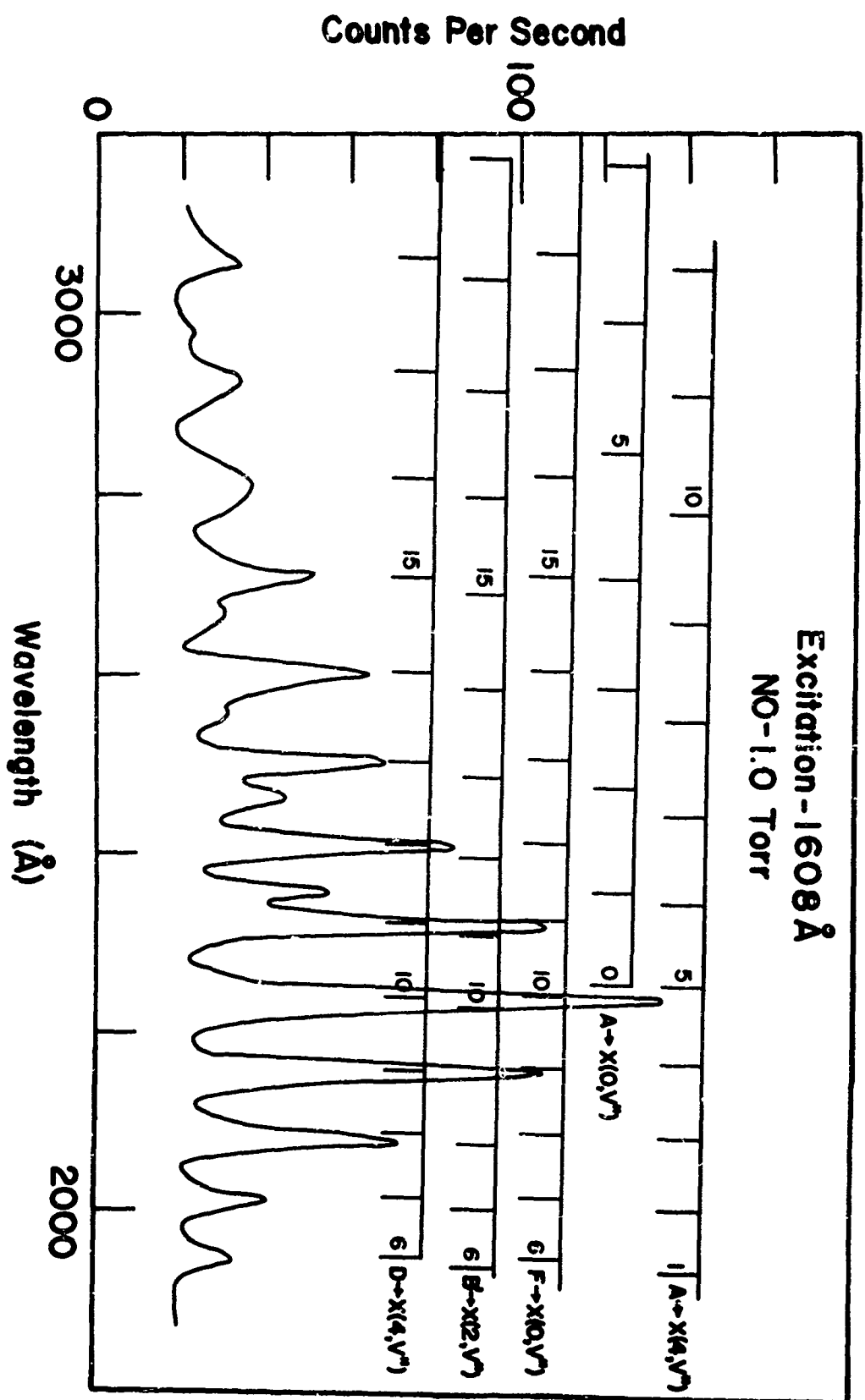


Fig. 4 (Sec. 3.7). NO fluorescence excited by 1608 Å.

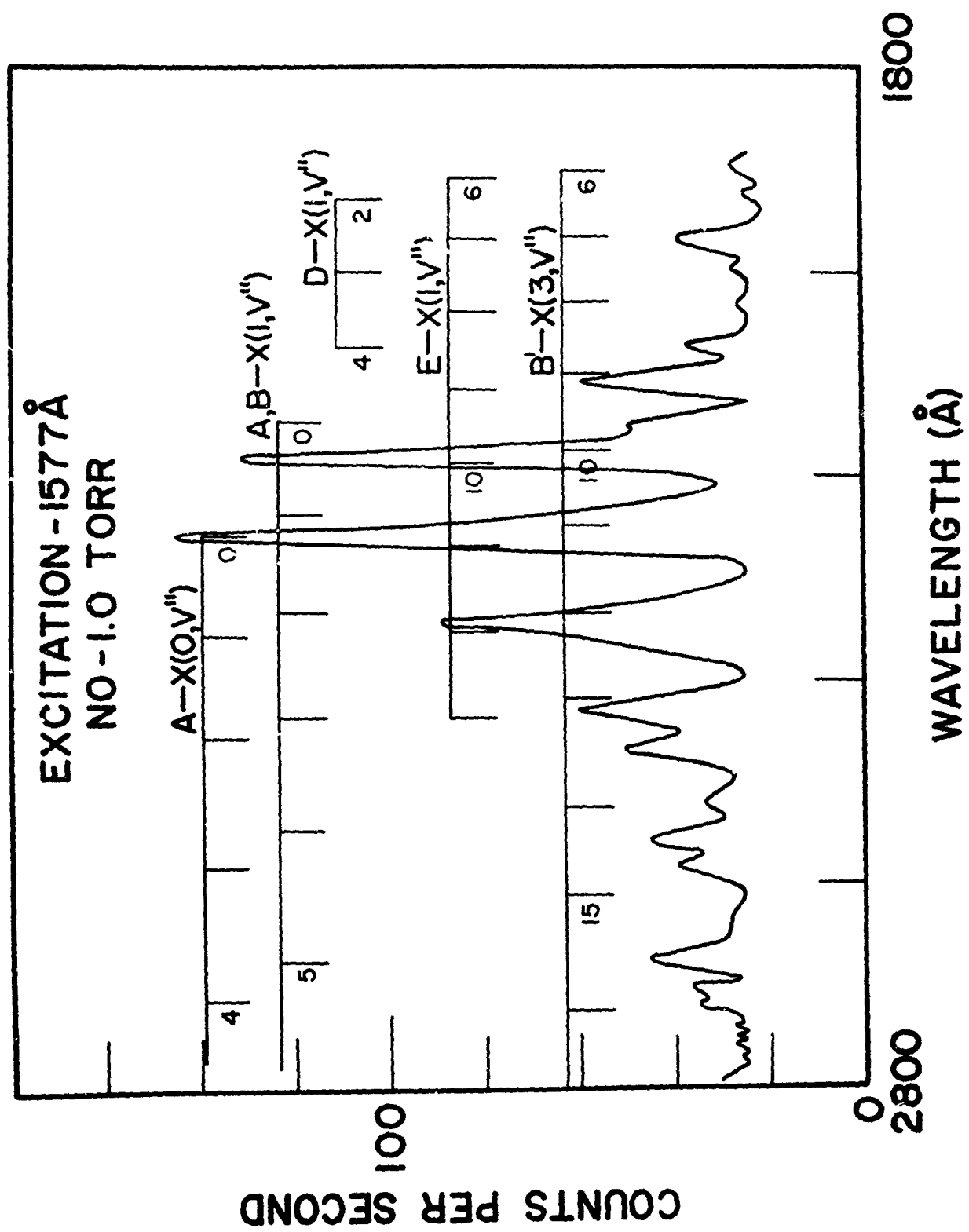


Fig. 5 (Sec. 3.7). NO fluorescence excited by 1577 Å.

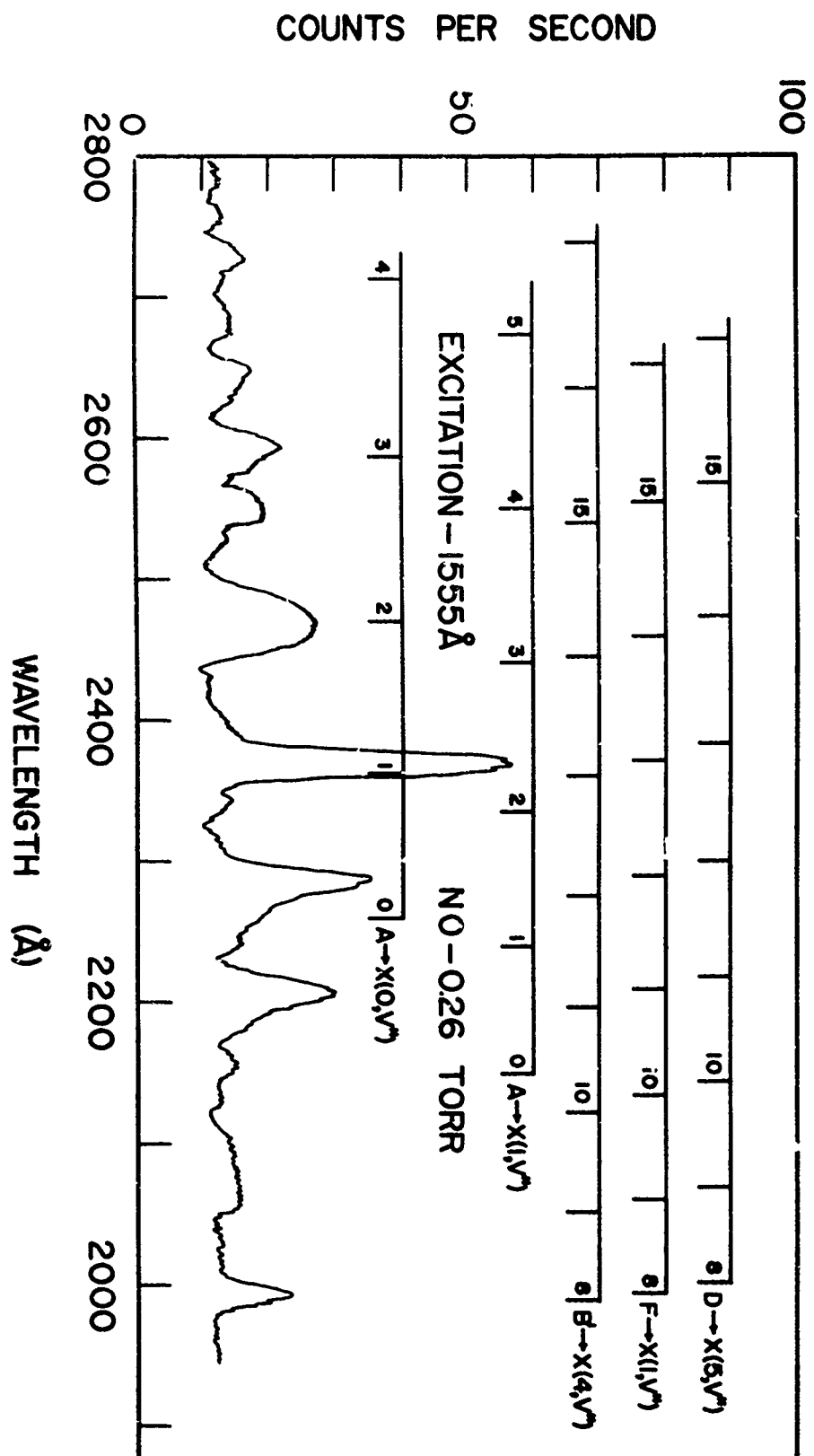


Fig. 6 (Sec. 3.7). NO fluorescence excited by 1555 Å.

Table I. NO Transitions.\*

A. Populated Upper States (2300 to 1400 Å):

$A^2\Sigma^+$ ,  $B^2\Pi$ ,  $C^2\Pi$ ,  $D^2\Sigma^+$ ,  $E^2\Sigma^+$ ,  $B'^2\Delta$ ,  $F^2\Delta$ ,  $N^2\Delta$ ,  $H^2\Sigma^+$ ,  $H'^2\Pi$ ,  $O^2\Sigma^+$ ,  
 $O'^2\Pi$ ,  $K^2\Pi$ ,  $M^2\Sigma^+$ ,  $S^2\Sigma^+$ .

B. Allowed Transitions:

$A \longrightarrow X$  ( $\gamma$  system)  
 $B \longrightarrow X$  ( $\beta$  system)  
 $C \longrightarrow X$  ( $\delta$  system),  $C \longrightarrow A$  (Heath system)  
 $D \longrightarrow X$  ( $\epsilon$  system),  $D \longrightarrow A$  (Feast #1 system)  
 $E \longrightarrow X$  ( $\gamma'$  system),  $E \longrightarrow A$  (Feast #2 system),  
 $E \longrightarrow C$ ,  $E \longrightarrow D$   
 $B' \longrightarrow X$  ( $\beta'$  system),  $B' \longrightarrow B$  (Ogawa system)  
 $F \longrightarrow X$ ;  $F \longrightarrow B$ ,  $F \longrightarrow C$ ,  
 $H, H' \longrightarrow X$ ;  $H, H' \longrightarrow A$ ,  $H, H' \longrightarrow C$ ,  $H, H' \longrightarrow D$   
 $O, O' \longrightarrow X$ ;  $O, O' \longrightarrow A$ ,  $O, O' \longrightarrow C$ ,  $O, O' \longrightarrow D$   
 $N \longrightarrow X$ ;  $N \longrightarrow B$ ,  $N \longrightarrow C$   
 $K \longrightarrow X$ ;  $K \longrightarrow A$ ,  $K \longrightarrow C$ ,  $K \longrightarrow D$   
 $M \longrightarrow X$ ;  $M \longrightarrow A$ ,  $M \longrightarrow C$ ,  $M \longrightarrow D$   
 $S \longrightarrow X$ ;  $S \longrightarrow A$ ,  $S \longrightarrow C$ ,  $S \longrightarrow D$

\* reference no. 1.

Table II. NO spectrum produced by 1640 Å radiation.

$\lambda(\text{\AA})$	$D \longrightarrow X$	$E \longrightarrow X$	$B^2 \longrightarrow X$	$A \longrightarrow X$
1945	(0, 1)			
1992		(0, 6)	(1, 6)	
2018	(0, 2)			
2063		(0, 7)	(1, 7)	
2096	(0, 3)			
2137		(0, 8)	(1, 8)	
2180	(0, 4)			
2215		(0, 9)	(1, 9)	
2265	(0, 5)			(0, 0)
2298		(0, 10)	(1, 10)	
2365				(0, 1)
2475				(0, 2)
2590				(0, 3)
2720				(0, 4)

Table III. NO spectrum produced by 1610 Å radiation.

$\lambda(\text{Å})$	$F \rightarrow X$	$D \rightarrow X$	$B' \rightarrow X$	$A \rightarrow X$
1950	(0, 6)	(4, 6)	(2, 6)	(4,1)
2018	(0, 7)	(4, 7)	(2, 7)	(4,2)
2089	(0, 8)	(4, 8)	(2, 8)	(4,3)
2163	(0, 9)	(4, 9)	(2, 9)	
2170				(4,4)*
2242	(0, 10)	(4, 10)	(2, 10)	
2262				(4,5)*(0,0)*
2325	(0, 11)	(4, 11)	(2, 11)	
2360				(4,6)*(0,1)*
2413	(0, 12)	(4, 12)	(2, 12)	
2450				(4,7)*
2470				(0,2)
2506	(0, 13)	(4, 13)	(2, 13)	
2552				(4,8)
2605	(0, 14)	(4, 14)	(2, 14)	(0,3)
2665				(4,9)
2710	(0, 15)	(4, 15)	(2, 15)	(0,4)
2785				(4,10)
2821	(0, 16)	(4, 16)	(2, 16)	
2850				(0,5)
2925	(0, 17)	(4, 17)	(2, 17)	(4,11)
3060	(0, 18)	(4, 18)	(2, 18)	

\* on shoulder of line, unresolved.

Table IV. NO spectrum produced by 1580 Å resolution.

$\lambda(\text{\AA})$	$B' \rightarrow X$	$E \rightarrow X$	$B \rightarrow X$		$D \rightarrow X$
			$A \rightarrow X$	$A \rightarrow X$	
1905	(3, 6)	(1, 6)			
1970	(3, 7)	(1, 7)			
2000					(1, 3)
2035	(3, 8)	(1, 8)			
2075					(1, 4)
2105	(3, 9)	(1, 9)			
2155			(1, 0)		
2180	(3, 10)	(1, 10)			
2240			(1, 1)*		
2260	(3, 11)	(1, 11)		(0, 0)	
2342	(3, 12)	(1, 12)	(1, 2)*	(0, 1)*	
2430	(3, 13)	(1, 13)	(1, 3)		
2470				(0, 2)	
2520	(3, 14)	(1, 14)			
2555			(1, 4)		
2590				(0, 3)	
2625	(3, 15)	(1, 15)			
2670			(1, 5)		
2715	(3, 16)	(1, 16)		(0, 4)	
2800			(1, 6)		
2815	(3, 17)	(1, 17)		(0, 5)	
2940	(3, 18)	(1, 18)	(1, 7)		

\* on shoulder of line, unresolved.

Table V. NO spectrum produced by 1550 Å radiation.

$\lambda(\text{\AA})$	$B' \rightarrow X$	$F \rightarrow X$	$D \rightarrow X$	$\begin{matrix} B \rightarrow X \\ A \rightarrow X \end{matrix}$	$A \rightarrow X$
1990	(4, 8)	(1, 8)	(5, 8)		
2055	(4, 9)	(1, 9)	(5, 9)		
2125	(4, 10)	(1, 10)	(5, 10)		
2150				(1, 0)	
2200	(4, 11)	(1, 11)	(5, 11)		
2240				(1, 1)*	
2262					(0, 0)*
2277	(4, 12)	(1, 12)	(5, 12)		
2335				(1, 2)	
2365	(4, 13)	(1, 13)	(5, 13)		(0, 1)
2470	(4, 14)	(1, 14)	(5, 14)	(1, 3)*	(0, 2)
2550	(4, 15)	(1, 15)	(5, 15)	(1, 4)	
2590					(0, 3)
2635	(4, 16)	(1, 16)			
2670				(1, 5)	
2715					(0, 4)

\* on shoulder of line, unresolved.



Table VI. Comparison of Franck-Condon factors for  
 $\text{NO } D^2\Sigma^+ \rightarrow X^2\Pi$ , and  $B'^2\Delta \rightarrow X^2\Pi$ .

$D \rightarrow X$	$\lambda(\text{\AA})$	$q_{v',v''} \text{ exp.}$	$q_{v',v''} \text{ theory}^a$
(0, 1)	1945	$0.34 \pm 0.10$	0.35
(0, 2)	2018	$0.28 \pm 0.09$	0.31
(0, 3)	2095	$0.23 \pm 0.06$	0.21
(0, 4)	2176	$0.15 \pm 0.04$	0.13
(1, 3)	2000	$0.46 \pm 0.14$	0.35
(1, 4)	2075	$0.54 \pm 0.11$	0.65

$B' \rightarrow X$	$\lambda(\text{\AA})$	$q_{v',v''} \text{ exp.}$	$q_{v',v''} \text{ theory}^a$
(1, 6)	1985	$0.33 \pm 0.09$	0.34
(1, 7)	2055	$0.36 \pm 0.07$	0.33
(1, 8)	2128	$0.14 \pm 0.06$	0.21
(1, 9)	2206	$0.11 \pm 0.04$	0.09
(1, 10)	2288	$0.06 \pm 0.03$	0.03

a. reference 14.

References

1. J. Heiklen and N. Cohen, *Advances in Photochemistry* 5, 157 (1968).
2. F. Ackermann and E. Miescher, *Chem. Phys. Letters* 2, 351 (1968).
3. F. Ackermann and E. Miescher, *J. Mol. Spectry* 31, 400 (1969).
4. R. Suter, *Cand. J. Phys.* 47, 881 (1969).
5. C. Jungen and E. Miescher, *Cand. J. Phys.* 47, 1769 (1969).
6. C. Jungen, *Cand. J. Phys.* 44, 3197 (1966).
7. F. R. Gilmore, *J. Q. S. R. T.* 5, 369 (1965).
8. C. Jungen and E. Miescher, *Astrophys. J.* 143, 1660 (1965).
9. A. B. Callear and I. W. M. Smith, *Trans. Fara. Soc.* 59, 1720 (1963).
10. R. A. Young, G. Black, and T. G. Slanger, *J. Chem. Phys.* 48, 2067 (1968).
11. H. Okabe, *J. Chem. Phys.* 47, 101 (1967).
12. K. L. Wray, *J. Q. S. R. T.* 2, 255 (1969).
13. H. A. Ory, *J. Chem. Phys.* 40, 562 (1964).
14. R. W. Nicholls, *J. Res. N. B. S.* 68A, 535 (1964).
15. R. J. Spindler, L. Isaacson, and T. Wentink, *J. Q. S. R. T.* 10, 621 (1970).
16. M. Huber, *Helv. Phys. Acta* 37, 329 (1964).

3.8 Hydrogen, Nitrogen, Oxygen, and Sulfur Dioxide

In the region 1125 to 1050 Å there are weak absorption bands corresponding to  $H_2$  ( $B^1\Sigma \leftarrow X^1\Sigma$ ) and  $N_2$  ( $C^3\Pi \leftarrow X^1\Sigma^+$ ) transitions. VUV scattering was observed for  $H_2$  ( $B^1\Sigma \rightarrow X^1\Sigma$ ), where  $v' = 0$  to 4. Nicholls<sup>1</sup> has computed Franck-Condon factors for these transitions. Total emission data was obtained with a sodium salicylate coated photomultiplier and the results are listed in Table 1, where the ratio of the maximum total uv emission intensity to the incident intensity ( $I_f/I_o$ ) is equal to unity. The absorption cross section was measured with 1 Å resolution to be  $1.5 \times 10^{-20} \text{ cm}^2$  for the  $B^1\Sigma \leftarrow X^1\Sigma$  (0,0) transition.

The radiative decay of the  $C^2\Pi$  state of  $N_2$  gives rise to the Second Positive ( $2^+$ ) bands of  $N_2$  ( $C^3\Pi \rightarrow B^3\Pi$ ), which in turn cascades to the  $A^3\Pi$  states with the emission of the First Positive ( $1^+$ ) bands. The emission of the  $2^+$  bands are in the 3000 to 4000 Å and the  $1^+$  bands in the 10,000 Å region. Relative intensity distribution of the  $C \rightarrow B$  (0, $v''$ ) and (1, $v''$ ) transitions were obtained. Fig. 1 shows the  $2^+$  (0, $v''$ ) transitions. Franck-Condon factors were calculated and compared with theoretical values<sup>2</sup> in Table 2. Nicholls<sup>3</sup> has calculated Einstein A coefficients with the use of relative emission data from an electrical discharge,<sup>4</sup> and the lifetimes of the vibrational levels of the  $C^3\Pi$  state obtained by Bennett and Dalby.<sup>5</sup> The calculated Franck-Condon factors<sup>2</sup> were used to place the relative band

strengths on an absolute basis. The present results are in good agreement with the theory and confirms the results of Nicholls.<sup>3</sup> Recently, Jeunehomme<sup>6</sup> repeated lifetime measurements of the C and B levels and obtained oscillator strengths for the  $2^+$  system which are in excellent agreement with Nicholls.<sup>3</sup> In the 1450 to 1150 Å region where the Lyman-Birge-Hopfield system ( $a^1\Pi_g - X^1\Sigma_g^+$ ) lie no detectable emission was observed.

In the case of  $O_2$  the emission curves showed no detectable emission for the Schumann-Runge bands ( $B^3\Sigma_u^- \rightarrow X^1\Sigma_g^-$ ). This is in agreement with the investigation of Hudson and Carter,<sup>7</sup> who found that the upper levels of  $B^3\Sigma_u^- v' = 3$  to 17 were predissociated. Tohmatsu<sup>8</sup> also reported no detectable emission of the Schumann-Runge bands in the earth's dayglow. Due to the spectral response of the EMI - 6255S photomultiplier the  $O_2$  ( $b^1\Sigma_g^+ \rightarrow X^3\Sigma_g^-$ ) emission at 7618 Å was not detected. Young, et al<sup>10</sup> and Filseth, et al,<sup>11</sup> investigated this emission excited by VUV radiation in the 1050 to 1700 Å region.

Emission from the  $\tilde{C}$  and  $\tilde{D} \leftrightarrow \tilde{X}$  transitions were observed for  $SO_2$ . The emission spectrum corresponded to the absorption coefficient curve of Golomb, et al.<sup>9</sup>

Table 1. Relative Emission Intensity for  $B^1\Sigma \rightarrow X^1\Sigma$  of  $H_2$ .

$v', v''$	$\lambda^*(A)$	$I_s/I_o$	Absorption cross section
0, 0	1108.6	1.00	$1.5 \times 10^{-20} \text{ cm}^2$
1, 0	1092.6	0.81	
2, 0	1077.6	0.72	
3, 0	1063.3	0.20	
4, 0	1049.7	0.10	

\* T. Namioka, J. Chem. Phys. 43, 1636 (1965).

Table 2. Comparisons of Franck-Condon factors for  $N_2$   
 $(C^3\Pi \longrightarrow B^3\Pi)$  Second Positive Bands.

$v', v''$	$q_{v', v''}$ exp.	$q_{v', v''}$ theory <sup>a</sup>
0, 0	$0.43 \pm 0.09$	0.46
0, 1	$0.33 \pm 0.08$	0.34
0, 2	$0.17 \pm 0.05$	0.15
0, 3	$0.07 \pm 0.04$	0.05
1, 0	$0.42 \pm 0.15$	0.48
1, 1	$0.02 \pm 0.03$	0.02
1, 2	$0.28 \pm 0.14$	0.25
1, 3	$0.28 \pm 0.14$	0.25

a. reference 2.

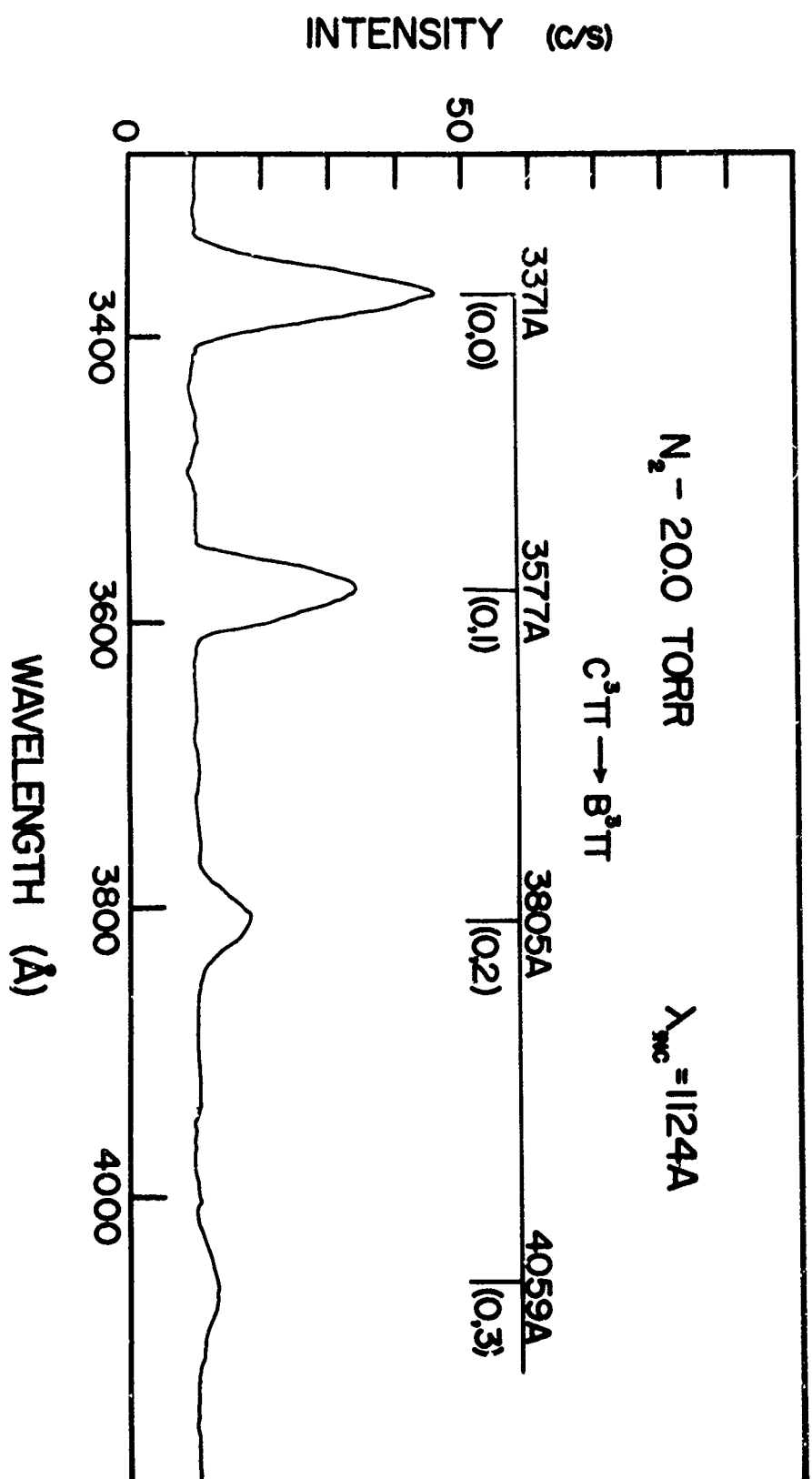


Fig. 1 (Sec. 3.8).  $N_2$  fluorescence - 2nd positive bands.

### References

1. R. W. Nicholls, *Astrophys. J.* 141, 819 (1965);  
R. J. Spindler, Jr., *J. Q. S. R. T.* 2, 597 (1969).
2. R. W. Nicholls, *J. of Res. N. B. S.* 65A, 451 (1961).
3. R. W. Nicholls, *J. Atmosph. Terr. Phys.* 25, 218 (1963).
4. L. V. Wallace and R. W. Nicholls, *J. Atmosph. Terr. Phys.* 24, 749 (1962).
5. R. G. Bennett and F. W. Dalby, *J. Chem. Phys.* 31, 434 (1957).
6. M. Jeunehomme, *J. Chem. Phys.* 44, 2672 (1966).
7. A. W. Johnson and R. G. Fowler, *J. Chem. Phys.* 53, 65 (1970).
8. R. D. Hudson and V. L. Carter, *Can. J. Phys.* 47, 1840 (1969).
9. T. Tohmatsu, *J. of Geomagnetism and Geoelectricity*, 20, 315 (1968).
10. R. A. Young, G. Black, and T. G. Slanger; *J. Chem. Phys.* 48, 2067 (1968).
11. S. V. Filseth, A. Zia, and K. H. Welge; *J. Chem. Phys.* 52, 5502 (1970).
12. D. Golomb, K. Watanabe, and F. F. Marmo; *J. Chem. Phys.* 36, 958 (1962).



#### 4. EFFECT OF MOLECULAR COLLISIONS ON FLUORESCENCE

##### 4.1 Introduction

The effect of collisions on the fluorescence of atmospheric and planetary gases is of interest in planetary ultraviolet spectroscopy. Since the gamma band emission of NO has been observed in the day glow of the earth,<sup>1</sup> the study of the collision of N<sub>2</sub> with excited NO is desirable. Laboratory studies on NO fluorescence in the presence of N<sub>2</sub> were made recently by Callear and Smith.<sup>2</sup> The D, C, and A electronic states of NO were populated with radiation from a xenon lamp and the fluorescence of these states was observed with a spectrometer. When N<sub>2</sub> was added the D and C state fluorescences were quenched while the A state (gamma band) fluorescence was enhanced. The C to A collision induced transition was found to be predominant and this added population of the A state explained the increase of gamma fluorescence. The diagram in Fig. 1 of section 3.7 shows the energy states of NO.

Callear<sup>3</sup> reviewed the possible types of energy transfer mechanisms involving the four types of molecular energy: translational, rotational, vibrational, and electronic. Two experimental investigations on electronic-electronic energy transfer of diatomic molecules have been reported.<sup>2,4</sup> Further study on NO-N<sub>2</sub> can be made by increasing the energy of the exciting radi-

ation to populate higher electronic states of NO, e. g. D, E, B, B', F states.<sup>5</sup> Many of these states may populate the C state by radiative transition or by level crossing.<sup>6</sup> This means that the fluorescence from the higher states could be affected by the NO-N<sub>2</sub> collisions.

With the use of monochromatic light, specific electronic states can be excited and the resulting fluorescence can be observed. Since a repulsive state<sup>7</sup> interacts with B, D, and E states, it would be worthwhile to investigate the fluorescence from B' and F states in the presence of N<sub>2</sub> and other gases.

#### 4.2 Inelastic Collisions and Quenching

The depopulation of excited states by inelastic collisions with ground state atoms or molecules may be expressed by

$$-\frac{dN_u}{dt} = N_u (\tau_u^{-1} + Z),$$

where  $N_u$  is the number of excited states per unit volume, and  $\tau_u$  the radiative lifetime of the excited state. The quantity  $Z$  is given by

$$Z = N \sigma_c V_r (\text{sec}^{-1}),$$

where  $N$  is the total particle density,  $V_r$  the mean relative velocity  $V_r = (16k_B T / \pi M)^{1/2}$ , with  $k_B$  the Boltzmann constant,  $M$  the atomic mass of the particle,  $T$  the temperature of the gas, and  $\sigma_c$  the cross section for inelastic collisions.<sup>8</sup>

In the collision deexcitation process with a quenching gas, the rate of forming the excited state is equal to the rate of depopulating the excited state under steady state conditions. Accordingly,

$$F = \frac{N_u}{\tau_u} + ZN_u.$$

Hence,

$$N_u = \frac{F}{\frac{1}{\tau_u} + Z}.$$

F must be independent of the foreign gas pressure and remain constant with the absorbing gas pressure and exciting radiation. The emitted radiation with the foreign (quenching) gas is equal to  $N_u/\tau_u$  or

$$\frac{N_u}{\tau_u} = \frac{F}{1 + \tau_u Z}.$$

Now, the emitted radiation without the foreign gas is equal to F; therefore, the quenching Q is defined by

$$Q = \frac{\text{Emission with foreign gas}}{\text{Emission without foreign gas}} = \frac{1}{1 + \tau_u Z}.$$

This equation was first obtained by Stern and Volmer.<sup>9</sup> Since Z varies linearly with foreign gas pressure P, a quenching curve of  $1/Q$  versus P should result in a straight line since

$$\frac{1}{Q} = 1 + \text{const. } P.$$

#### 4.3 Effect of $N_2$ and Argon on Fluorescence of NO

The excitation wavelengths of 1640, 1610, 1580, and 1550 Å were used to excite NO to various upper states (see section 3.7). Figures 3, 4, 5, and 6 in section 3.7 show the typical fluorescence spectra of NO. In order to study the effects of  $N_2$  and argon on the fluorescence of NO, pressure of about 0.20 Torr of NO were used to minimize self absorption of the emission. The pressures of the quenching gases were varied from 0.20 to 100 Torr. As the pressure of  $N_2$  was increased, the fluorescence of NO except for the  $\gamma$  bands was quenched. The  $\gamma$  band intensity increased as the pressure of  $N_2$  was increased. A partial pressure of about 20 Torr of  $N_2$  was sufficient to quench the emission of NO except for the  $A^2E^+$  state. When argon was used as the quenching gas, the NO fluorescence decreased with the increase of argon pressure. The  $A^2E^+$  state was also quenched and this is in agreement with the interpretation that the A state was formed by radiative decay from the upper states and not by direct excitation with the wavelengths used. Figures 1 and 2 illustrate Stern-Volmer plots for NO emission quenched by  $N_2$  and argon. The curves are in agreement with the collisional deactivation model. The slopes show that the quenching effect of  $N_2$  is greater than that of argon. Figure 3 shows the enhancement

of the  $\gamma(0,1)$  band as  $N_2$  is added to NO. The curve shows a gradual rise of the intensity with pressures greater than 20 Torr of  $N_2$ . The fluorescence spectrum of excited NO with  $N_2$  pressures greater than 20 Torr is primarily due to  $\gamma$  bands. A trace of the  $\gamma$  bands is shown in Figure 4. Since the  $\gamma$  bands were isolated, the Franck-Condon factors were obtained with  $N_2$  pressures ranging from 23 to 100 Torr. The results are tabulated in Table I, and are in good agreement with theoretical values. The  $\gamma(0,0)$  band was affected by self absorption and was not included in the comparison. The  $\gamma(0,1)$  band may be slightly affected by self absorption due to Boltzmann population of  $v'' = 1$  of the ground state of NO. A slightly higher  $q_{0,1}$  may result if corrections for self absorption were made.

According to the calculated Franck-Condon factors,<sup>10</sup> the  $\epsilon$ ,  $\gamma'$ ,  $F \rightarrow X$ , and  $K \rightarrow X$  systems should be intense in the region less than  $2000 \text{ \AA}$ . The non Rydberg state  $B'$  should radiate strongly in the region 2000 to  $3000 \text{ \AA}$ . The emission observed in the present investigation are probably due to  $\beta'$  bands with small overlapping contributions from  $\epsilon$ ,  $\gamma'$  and  $F \rightarrow X$  bands. Although the emissions less than  $1900 \text{ \AA}$  were not monitored, we infer that the  $\beta'$ ,  $\epsilon$ ,  $\gamma'$  and  $F \rightarrow X$  emissions  $v'' < 6$  are also quenched by  $N_2$  and argon.

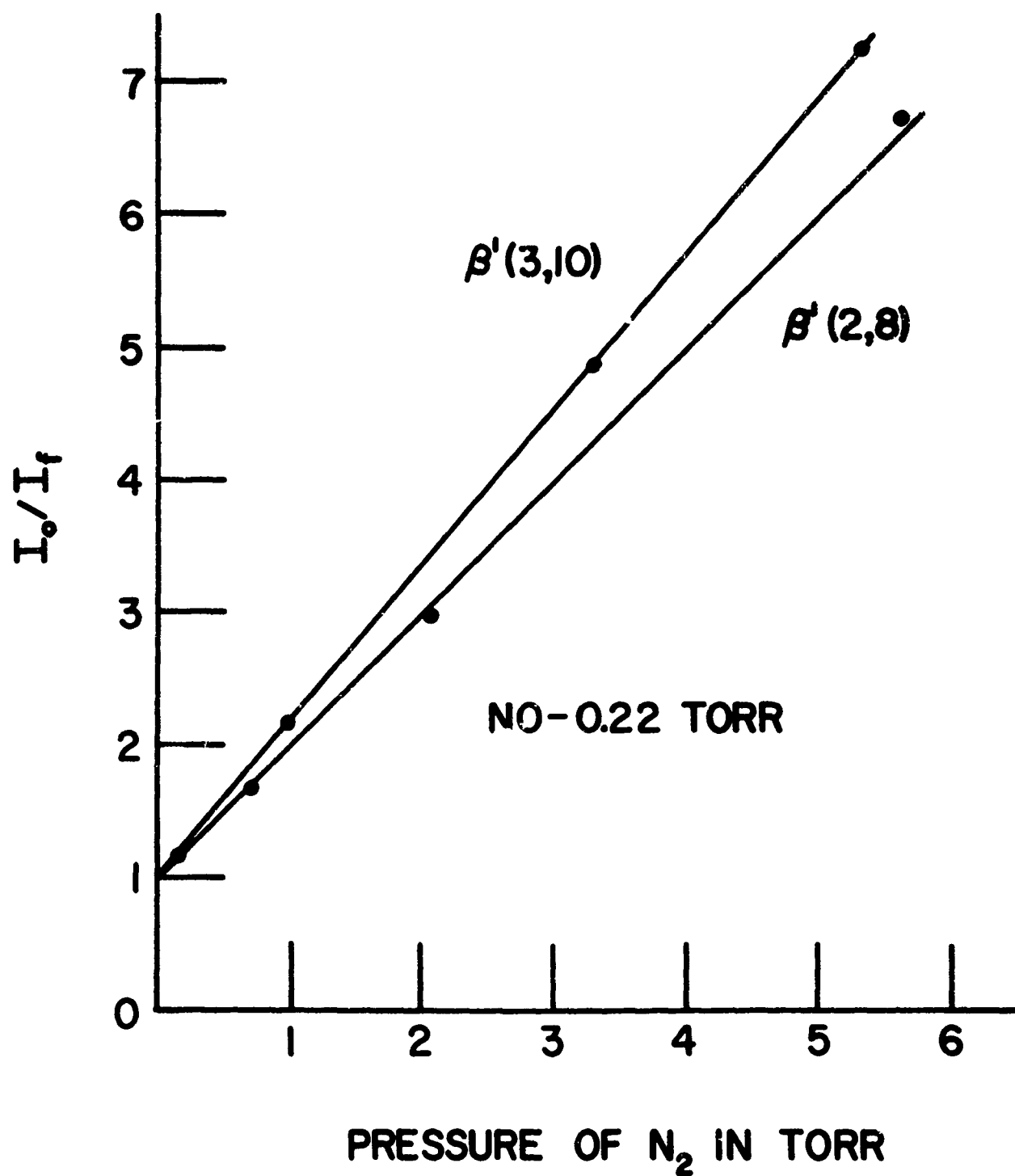


Fig. 1 (Sec. 4.3). Stern-Volmer plot for quenching by  $N_2$ .

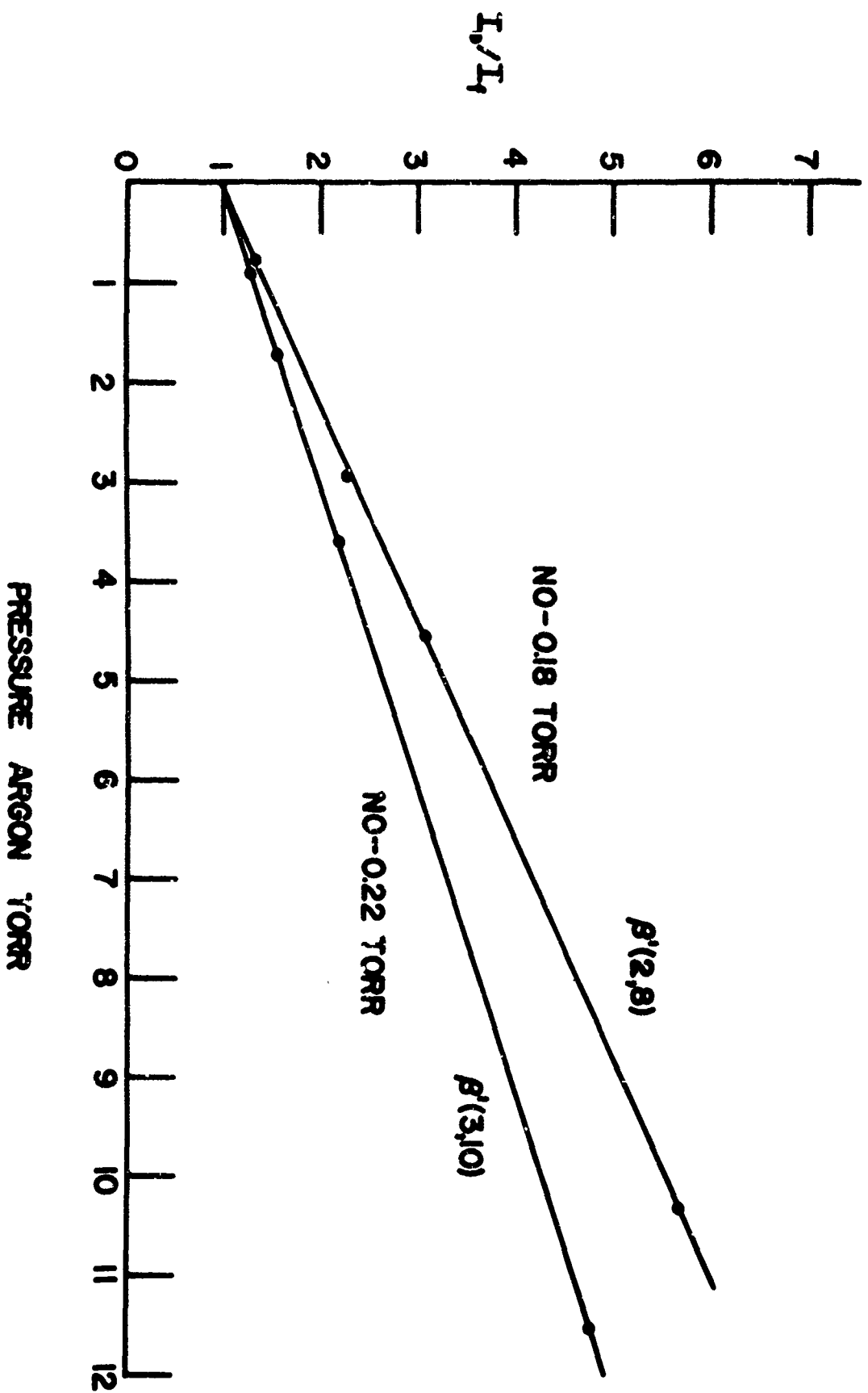


Fig. 2 (Sec. 4.3). Stern-Volmer plot for quenching by argon.

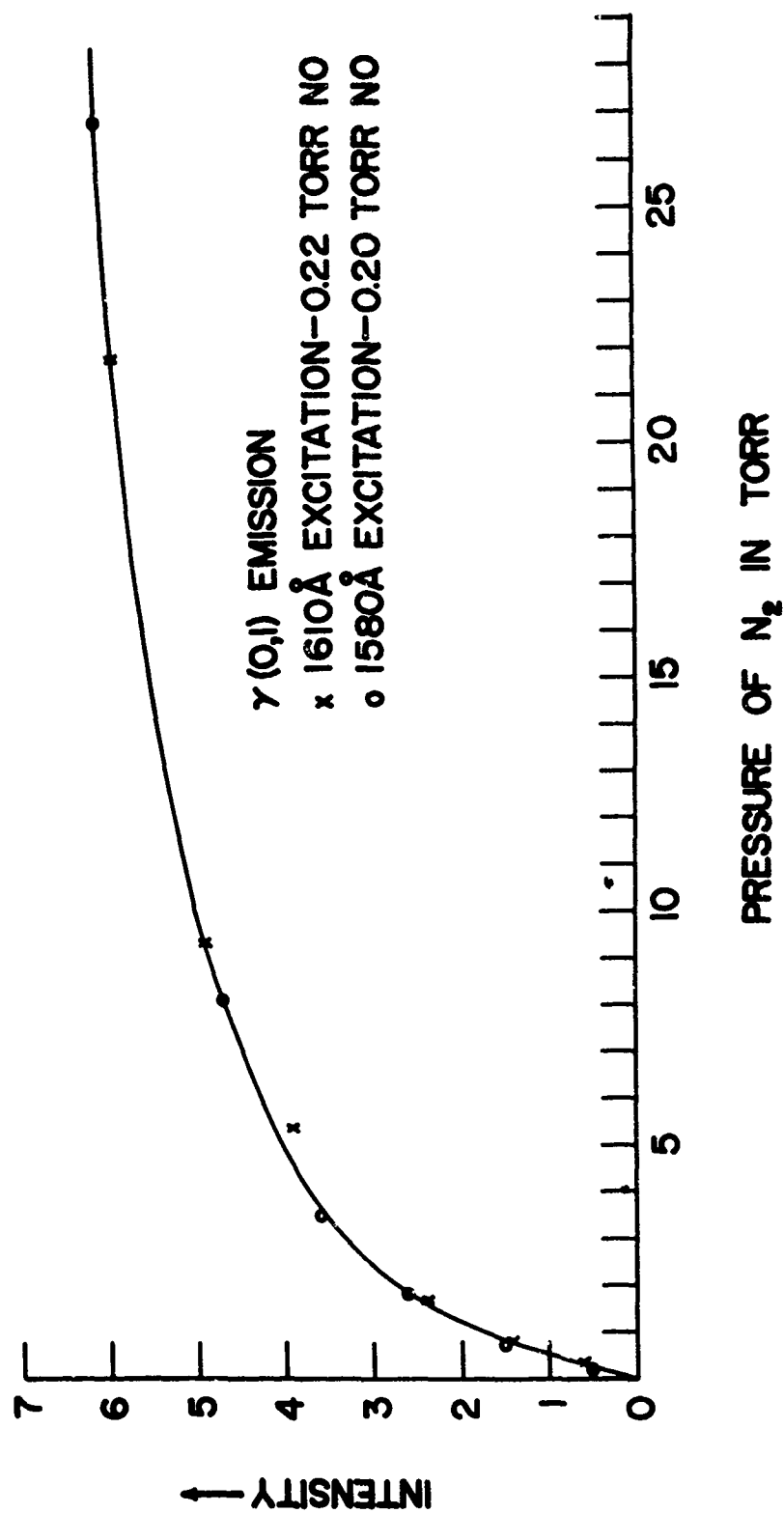


Fig. 3 (Sec. 4.3). NO gamma band enhancement with the addition of N<sub>2</sub>.



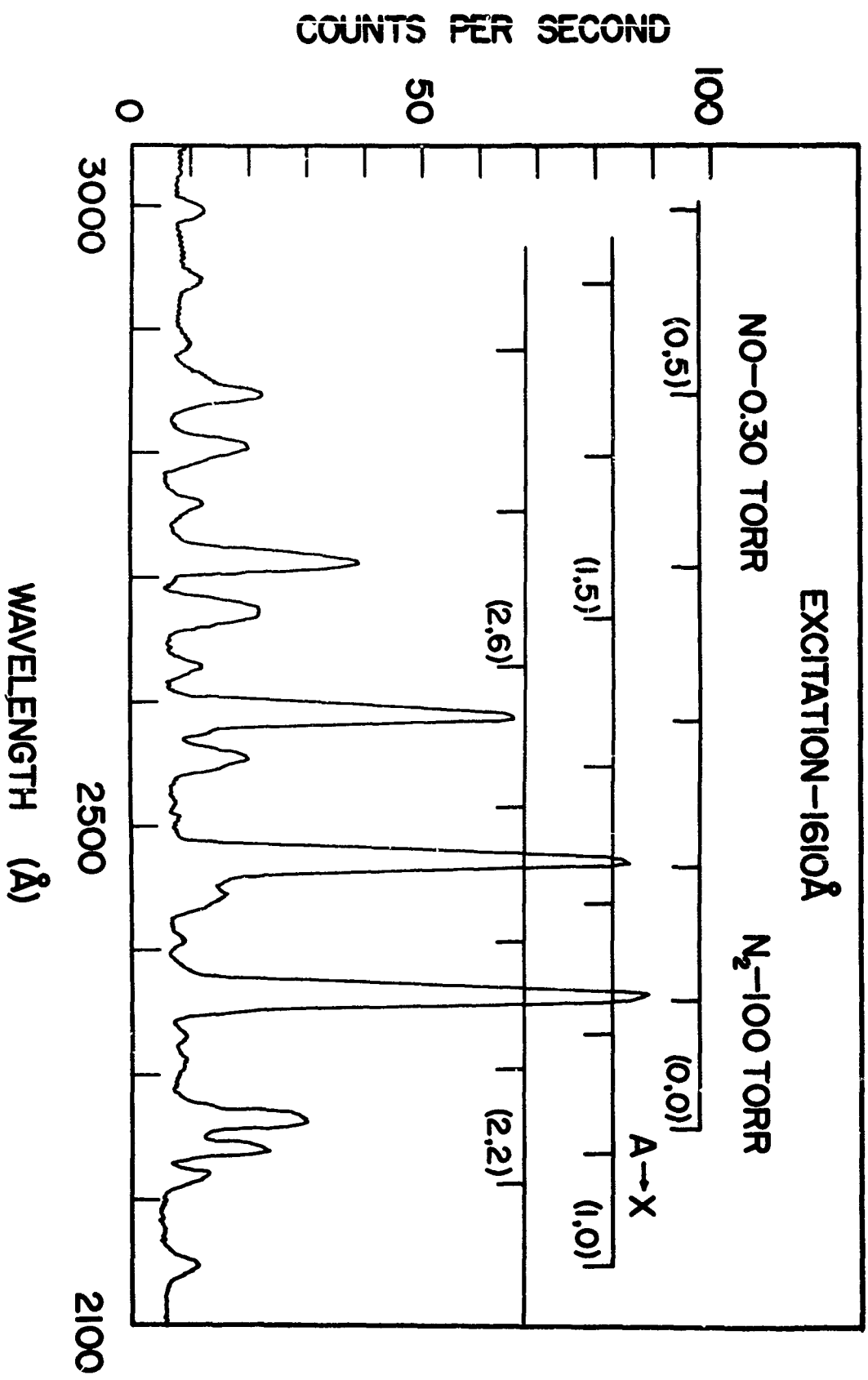


Fig. 4 (Sec. 4.3). Spectrum of NO gamma bands induced by N<sub>2</sub> collisions.

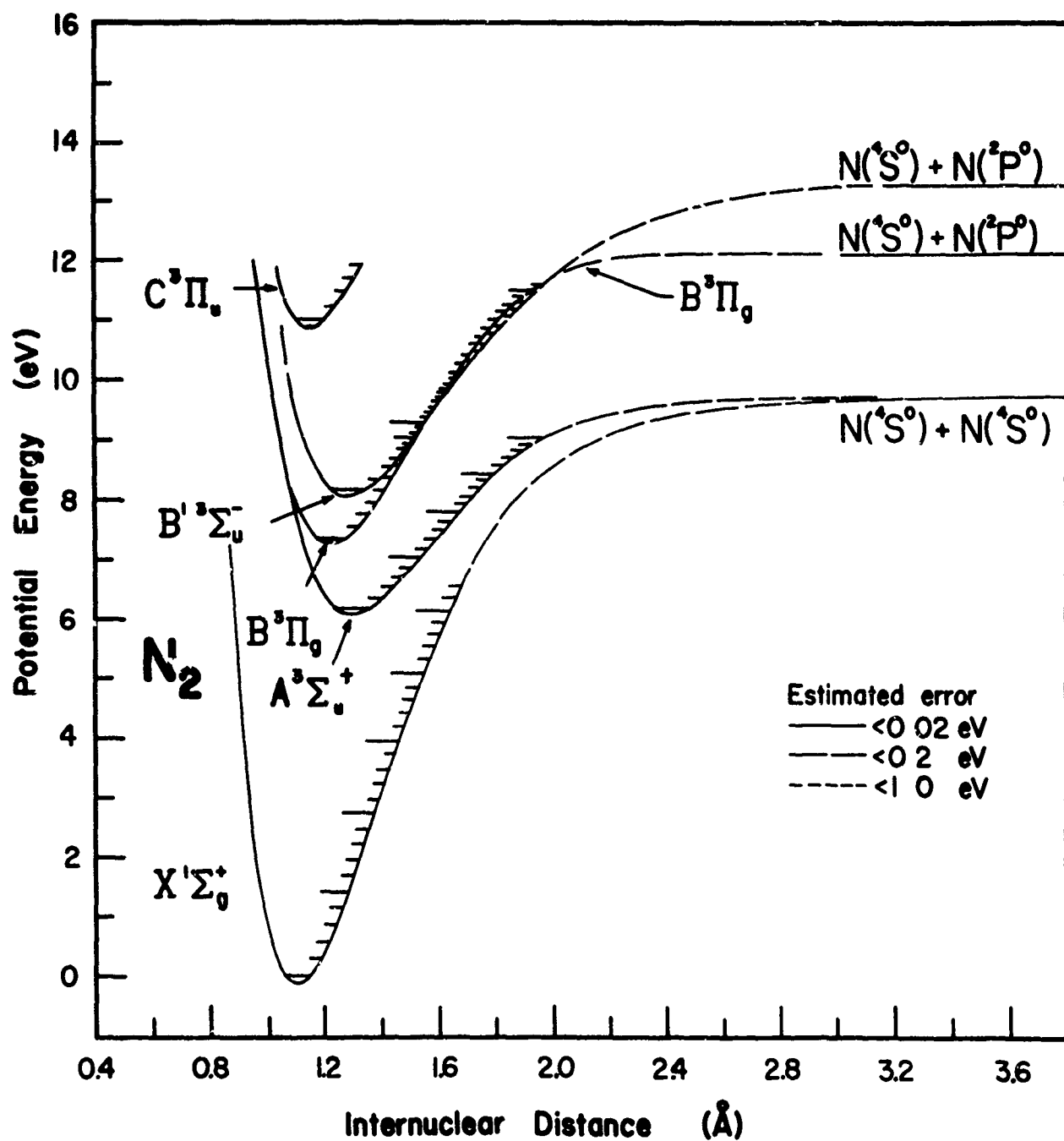


Fig. 5 (Sec. 4.3). Potential energy diagram of  $N_2$  (F. R. Gilmore, J.Q.S.R.T. 2, 369 (1964)).

Table I. NO gamma band emission in presence of  $N_2$ .

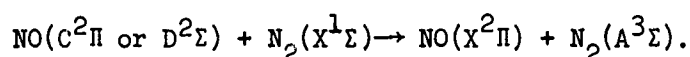
$v' \ v''$	$\lambda(\text{\AA})$	$q_{v',v''}$ exp.	$q_{v',v''}$ theory <sup>a</sup>
0, 1	2362	$0.29 \pm 0.03$	0.32
0, 2	2470	$0.27 \pm 0.03$	0.29
0, 3	2586	$0.22 \pm 0.02$	0.19
0, 4	2712	$0.12 \pm 0.02$	0.11
0, 5	2848	$0.07 \pm 0.01$	0.06
0, 6	2998	$0.03 \pm 0.01$	0.03

a. R. W. Nicholls, J. Res. N.B.S. 68A, 535 (1965)

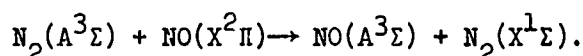
D. C. Jain and R. C. Sahni, Trans. Fara. Soc. 64, 3169 (1968)

R. J. Spindler, L. Isaacson, and T. Wentink, J.Q.S.R.T. 10,  
621 (1970)

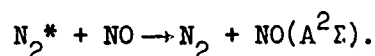
The quenching of the B', D, E, and F states with the enhancement of  $\gamma$  band emission can be explained by the collision mechanism proposed by Callear and Smith<sup>2</sup> for  $\delta$  ( $v = 0$ ) and Callear, Pilling and Smith<sup>11</sup> for  $\epsilon$  ( $v = 0$ ) quenching by  $N_2$ . They<sup>2,11</sup> established that the  $C \rightarrow A$ , and  $D \rightarrow A$  transitions occur via the intermediacy of  $N_2 A^3\Sigma^+$  as energy carrier. The collisional quenching mechanism can be described by



The enhancement of the  $\gamma$  band is attributed to the collision mechanism

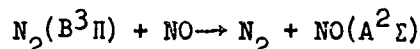


Since  $N_2(A^3\Sigma)$  has a relatively long radiative lifetime (0.9 sec<sup>12</sup> and 12 sec<sup>13</sup>), we may expect an efficient conversion of  $N_2(A^3\Sigma)$  to  $NO(A^2\Sigma)$ . Dugan<sup>14</sup> has shown that the metastable nitrogen  $N_2^*$  excited by low energy electron impact can produce the  $\gamma$  emission by collision with NO. The energy transfer mechanism is believed to be



The excited states of the NO molecule may have enough energy to collisionally excite the  $N_2$  ground state not only to the  $A^3\Sigma$  but the  $B^3\Pi$  state (see Fig. 5). Okabe<sup>15</sup> has suggested the

reaction



in his investigation of  $\gamma$  and  $\beta$  fluorescence in the photo-dissociation of  $\text{N}_2\text{O}$ . The lifetime of  $\text{N}_2(\text{B}^3\Pi \rightarrow \text{A}^3\Sigma)$  is about  $10^{-5}$  sec,<sup>16</sup> so this state should provide efficient collisional conversion for pressures  $>0.1$  Torr of  $\text{N}_2$ . Energy transfer from highly excited NO to  $\text{N}_2$  should populate the  $\text{B}^3\Pi$  state as well as the  $\text{A}^3\Sigma$  state of  $\text{N}_2$ .

In order to investigate the extent of the  $\gamma$  band enhancement in the presence of  $\text{N}_2$ , the Bausch and Lomb monochromator (20 Å bandwidth) was set at the  $\gamma(0,1)$  wavelength. The excitation radiation was varied with the McPherson monochromator (10 Å bandwidth) in the region 1350 to 2300 Å. Pure NO (0.20 Torr) and NO +  $\text{N}_2$  excitation spectra were obtained. The NO traces showed weak  $\gamma(0,1)$  emission at 1640, 1610, 1580, and 1550 Å, which is consistent with our results in section 3.7. When  $\text{N}_2$  was added (30 to 77 Torr), the excitation spectra showed C( $v = 0$  to 3), D( $v = 0$  to 3), B', E, F and other Rydberg states to 1370 Å emitting  $\gamma(0,1)$  radiation. The vibrational levels of B', D, E, F, and other Rydberg states overlapped but definite peaks in the region less than 1670 Å could be related to B'( $v = 0$  to 10). The non-Rydberg B state also showed weak  $\gamma(0,1)$  emission with 77 Torr of  $\text{N}_2$  for  $v = 9, 12$ . The

$v = 7, 8, 10$  and  $11$  vibrational levels of the B state overlapped with C and D levels. This is in agreement with the pressure broadened curve of Bethke.<sup>17</sup> The NO  $C^2\Pi(v > 0)$  and  $B^2\Pi(v > 7)$  states have not been observed in emission due to predissociation. Our observation implies that predissociation is inhibited for these levels by  $N_2$  collisions, thereby allowing  $C \rightarrow A$  and  $B \rightarrow A$  transitions to occur via the intermediacy of  $N_2A^3\Sigma$ .

References

1. C. Barth, J. Geophys. Res. 69, 3301 (1964).
2. A. B. Callear and I. W. M. Smith, Trans. Faraday Soc. 61, 2383 (1965).
3. A. B. Callear, "Photochemistry and Reaction Kinetics" (Sudgen, et al., eds.), p. 133, Cambridge Press, London, 1967.
4. N. H. Sagert and B. A. Thrush, Disc. Faraday Soc. 37, 223 (1964).
5. E. Miescher, J. Q. S. R. T. 2, 421 (1962).
6. M. Huber, Helv. Phys. Acta, 37, 329 (1964).
7. C. Jungen and E. Miescher, Astrophys. J. 142, 1660 (1965).
8. A. C. G. Mitchell and M. W. Zemansky, "Resonance Radiation and Excited Atoms," University Press, Cambridge, 1961.
9. O. Stern and M. Volmer, Phys. Zeits. 20, 183 (1919).
10. R. W. Nicholls, J. Research N.B.S., 68A, 535 (1964).
11. A. B. Callear, M. J. Pilling and I. W. M. Smith, Trans. Faraday Soc. 64, 1 (1968).
12. E. C. Zipf, J. Chem. Phys. 38, 2034 (1963).
13. W. Brennen, J. Chem. Phys. 44, 1793 (1966).
14. C. H. Dugan, J. Chem. Phys. 45, 87 (1966).
15. H. Okabe, J. Chem. Phys. 47, 101 (1967).
16. M. Jeunehomme and A. B. F. Duncan, J. Chem. Phys. 41, 1962 (1964).
17. G. W. Bethke, J. Chem. Phys. 31, 662 (1959).

## 5. CONCLUDING REMARKS

In our absorption and photoionization studies, we were able to identify several new Rydberg series and to determine the onset of dissociation continua. Most of our recent measurements were made with  $0.3 \text{ \AA}$  resolution and it would be worthwhile to continue the cross section measurements with higher resolution in the spectral region where the measured cross sections showed an apparent pressure effect.

The results of our fluorescence measurements indicate that some of the excited states cascaded to lower electronic states with emission of radiation. We were able to measure the emission of several gases over a limited spectral region (2000 to 6000  $\text{\AA}$ ). For CO,  $\text{N}_2$ , and NO, the measured Franck-Condon factors were found to be in good agreement with the calculated values. This suggests that the approximations made in the theoretical consideration of the radiative transitions are useful. Since the emissions appear also in the vacuum ultraviolet and the infrared regions, fluorescence measurements over a wider spectral region would be desirable. Further work in this area should determine the branching ratios for the radiative transitions.

In the study of the effect of molecular collisions on the fluorescence of NO, we observed the quenching and enhancement effect on certain emission bands. If the quenching of the B'



state of NO involves de-excitation of the NO molecule to its ground state, the energy transfer should populate the  $B^3\Pi$  state or the  $A^3\Sigma$  state of  $N_2$ . Accordingly, the enhancement of the  $\gamma$  band emission could be attributed to NO molecules excited to the  $A^2\Sigma$  state via collisions with the excited  $N_2$  molecules.

DOCUMENT CONTROL DATA - R&D		
(Security classification of title, body of abstract and indexing annotation must be entered when the overall report is classified)		
1. ORIGINATING ACTIVITY (Corporate author) Department of Physics and Astronomy University of Hawaii Honolulu, Hawaii 96822		2a. REPORT SECURITY CLASSIFICATION Unclassified
		2b. GROUP
3. REPORT TITLE  STUDY OF SCATTERING AND FLUORESCENCE OF GASES IN THE VACUUM ULTRAVIOLET		
4. DESCRIPTIVE NOTES (Type of report and inclusive dates) Scientific. Final: 1 April 1965 to 30 September 1970. Approved: 16 November 1970		
5. AUTHOR(S) (First name, middle initial, last name) Frederick M. Matsunaga Kenichi Watanabe William Pong (PI)		
6. REPORT DATE 30 October 1970	7a. TOTAL NO. OF PAGES 99	7b. NO. OF REFS 119
8a. CONTRACT OR GRANT NO. AF 19(628)-4967		9a. ORIGINATOR'S REPORT NUMBER(S)
b. PROJECT, TASK, WORK UNIT NOS. 8627-01-01		
c. DOD ELEMENT 61102F		9b. OTHER REPORT NO(S) (Any other numbers that may be assigned this report)
d. DOD SUBELEMENT 681310		AFCL-70-0615
10. DISTRIBUTION STATEMENT  This document has been approved for public release and sale; its distribution is unlimited.		
11. SUPPLEMENTARY NOTES  TECH, OTHER		12. SPONSORING MILITARY ACTIVITY Air Force Cambridge Research Laboratories (LK) L. G. Hanscom Field Bedford, Massachusetts 01730
13. ABSTRACT <p>Measurements of spectral absorption and photoionization cross sections of <math>\text{CO}_2</math>, <math>\text{NH}_3</math>, <math>\text{O}_2</math>, <math>\text{COS}</math>, <math>\text{NO}</math>, <math>\text{N}_2</math>, and vinyl chloride in the region 580 - 1650 Å were made. A number of new Rydberg series were found and the convergence limits were compared with the photoionization values.</p> <p>In the study of dispersed fluorescence from molecules, particular attention was given to the emissions from <math>\text{CO}</math>, <math>\text{NH}_3</math>, <math>\text{N}_2</math>, and <math>\text{NO}</math> in the spectral region 1800 to 6000 Å. The experimental Franck-Condon factors for <math>\text{CO}</math> and <math>\text{N}_2</math> were found to be in good agreement with the theoretical values. The threshold for the <math>\text{NH } c^1\Pi \rightarrow a^1\Delta</math> transition was observed at <math>(1245 \pm 10)</math> Å. On the basis of the observed threshold of the <math>\text{NH}</math> emission, the calculated energy separation of the <math>a^1\Delta</math> state from the ground state of <math>\text{NH}</math> is <math>(2.2 \pm 0.1)</math> eV which is somewhat higher than the value previously reported. The excitation spectra of <math>\text{NO}</math> show many overlapping states. However, the <math>\text{B}' \rightarrow \text{X}</math> transitions of <math>\text{NO}</math> were identified, and the experimental Franck-Condon factors are in agreement with the calculated values. The results suggest that the <math>\gamma'</math> band contribution in <math>\text{NO}</math> emission is negligible. The excitation spectra of other molecules such as <math>\text{H}_2</math>, <math>\text{O}_2</math>, and <math>\text{SO}_2</math> were studied, and certain features of the emission spectra can be related to the spectral absorption.</p> <p>The effect of molecular collisions on the fluorescence of <math>\text{NO}</math> was investigated. Quenching of the <math>\text{B}'</math>, <math>\text{D}</math>, <math>\text{E}</math>, and <math>\text{F}</math> states with the enhancement of the <math>\gamma</math> band emission was observed.</p>		

Unclassified

Security Classification

14. KEY WORDS	LINK A		LINK B		LINK C	
	ROLE	WT	ROLE	WT	ROLE	WT
Absorption coefficients Photoionization yields Vacuum ultraviolet Fluorescence Franck-Condon factors Energy transfer Carbon monoxide Ammonia Nitric oxide Molecular nitrogen Molecular hydrogen Molecular oxygen Sulfur dioxide						

Unclassified

Security Classification